

INVESTIGATION OF WAKE WASH IN TOWING TANK

RESEARCHERS:

IR. DR. MOHAMAD PAUZI ABDUL GHANI (HEAD)  
MOHD NOR ASHIKIN ABDUL RAHIM

RESEARCH VOT NO:  
75190

FAKULTI KEJURUTERAAN MEKANIKAL  
UNIVERSITI TEKNOLOGI MALAYSIA

2006

UNIVERSITI TEKNOLOGI MALAYSIA

BORANG PENGESAHAN  
LAPORAN AKHIR PENYELIDIKAN

TAJUK PROJEK : INVESTIGATION OF WAKE WASH IN TOWING TANK

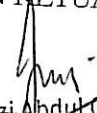
Saya MOHAMAD PAUZI ABDUL GHANI  
(HURUF BESAR)

Mengaku membenarkan Laporan Akhir Penyelidikan ini disimpan di Perpustakaan  
Universiti Teknologi Malaysia dengan syarat-syarat kegunaan seperti berikut :

1. Laporan Akhir Penyelidikan ini adalah hakmilik Universiti Teknologi Malaysia.
2. Perpustakaan Universiti Teknologi Malaysia dibenarkan membuat salinan untuk tujuan rujukan sahaja.
3. Perpustakaan dibenarkan membuat penjualan salinan Laporan Akhir Penyelidikan ini bagi kategori TIDAK TERHAD.
4. \* Sila tandakan ( / )

- |                                     |              |   |
|-------------------------------------|--------------|---|
| <input type="checkbox"/>            | SULIT        | (Mengandungi maklumat yang berdarjah keselamatan atau Kepentingan Malaysia seperti yang termaktub di dalam AKTA RAHSIA RASMI 1972). |
| <input type="checkbox"/>            | TERHAD       | (Mengandungi maklumat TERHAD yang telah ditentukan oleh Organisasi/badan di mana penyelidikan dijalankan).                          |
| <input checked="" type="checkbox"/> | TIDAK TERHAD |   |

TANDATANGAN KETUA PENYELIDIK

  
Dr Mohamad Pauzi Abdul Ghani, P.Eng  
Nunna & Co. Kejuruteraan Penyelidik  
Fakulti Kejuruteraan Penyelidik  
Universiti Teknologi Malaysia  
Jalan UTM Skudai, Johor  
81300 UTM Skudai, Johor  
01/06/2006

CATATAN : \* Jika Laporan Akhir Penyelidikan ini SULIT atau TERHAD, sila lampirkan surat daripada pihak berkenaan/organisasi berkenaan dengan menyatakan sekali sebab dan tempoh laporan ini perlu dikelaskan sebagai SULIT dan TERHAD.

**INVESTIGATION OF WAKE WASH IN TOWING TANK**

**RESEARCHERS:**

**IR. DR. MOHAMAD PAUZI ABDUL GHANI (HEAD)  
MOHD NOR ASHIKIN ABDUL RAHIM**

**RESEARCH VOT NO:  
75190**

**FAKULTI KEJURUTERAAN MEKANIKAL  
UNIVERSITI TEKNOLOGI MALAYSIA**

**2006**

“Saya akui laporan penyelidikan bertajuk “*Investigation of Wake Wash in Towing Tank*” adalah hasil kerja saya sendiri kecuali nukilan dan ringkasan yang tiap-tiap satunya telah saya jelaskan”

Tandatangan :  .....

Nama Penulis : **Mohamad Pauzi Abdul Ghani** .....

Tarikh : **1 June, 2006** .....

## INVESTIGATION OF WAKE WASH IN THE TOWING TANK

(Keywords: Wake wash, wave pattern, wave making resistance)

### ABSTRACT

In recent years, the demand for high speed craft has increased significantly. The wave resistance plays an important role in total resistance and power prediction, which influence the design. Additionally, wake wash generated by high-speed crafts is also important to the design concept due to its impact on safety and environment such as beach/bank erosion, risk to people on shore and small boats in harbours and changes in the local ecology.

This report describes about the investigation of wake wash developed from high speed marine craft in the towing tank. The data acquisition system and wave probe for wake wash measurement has been developed.

### Key researchers:

Ir. Dr. Mohamad Pauzi Abdul Ghani (Head)  
Mohd Nor Ashikin Abdul Rahim

Email: [pauzi@fkm.utm.my](mailto:pauzi@fkm.utm.my)  
Tel. No.: 607-5534760  
Fax. No.: 607-5566159

**KAJIAN HAKIS KERACAK (*WAKE WASH*) DI DALAM TANGKI TUNDA**  
(katakunci: hakis keracak, bentuk ombak, rintangan buatan ombak)

**ABSTRAK**

Masakini permintaan terhadap penggunaan kapal/bot berkelajuan tinggi telahpun meningkat. Bagi kapal/bot jenis ini, rintangan ombak memainkan peranan utama dan merupakan komponen utama di dalam rintangan total kapal/bot berkenaan yang mempengaruhi anggaran kuasa kapal/bot dan seterusnya mempengaruhi rekabentuk kapal/bot tersebut. Sebagai tambahan pada rintangan buatan ombak, hakis keracak daripada kapal/bot berkelajuan tinggi juga penting dan perlu diambilkira di dalam proses merekabentuk bentuk badan kapal/bot. Hakis keracak ini memberi impak yang besar terhadap ciri-ciri keselamatan dan alam sekitar, sebagai contoh seperti hakisan tebing dan pantai, memberhayakan pada bot-bot kecil dan orang ramai di pantai dan juga boleh merubah sistem ekologi tempatan.

Laporan ini menerangkan berkenaan dengan kajian hakis keracak dari kapal/bot berkelajuan tinggi di dalam tangki tunda dan dimasa yang sama sistem perolehan data dan pengukuran hakis keracak telahpun dibangunkan.

**Penyelidik Utama:**

Ir. Dr. Mohamad Pauzi Abdul Ghani  
Mohd Nor Ashikin Abdul Rahim

Email: [pauzi@fkm.utm.my](mailto:pauzi@fkm.utm.my)  
Tel. No.:607-5534760  
Fax. No.:607-5566159

## PENGHARGAAN

Para penyelidik ingin mengucapkan setinggi-tinggi penghargaan dan terima kasih kepada Universiti Teknologi Malaysia kerana membantu dalam menguruskan penyelidikan ini. Penyelidikan ini dibiayai di bawah skim jangka pendek melalui nombor projek 75190. Penghargaan dan terima kasih juga kepada pelajar-pelajar ijazah pertama dan sarjana dan juruteknik-juruteknik di atas bantuan dan idea yang diberikan sepanjang penyelidikan ini dijalankan. Akhir sekali terima kasih kepada Pusat Pengurusan Penyelidikan (RMC, UTM) dan Jawatankuasa Penyelaras Penyelidikan, Fakulti Kejuruteraan Mekanikal, UTM di atas segala pertolongan dalam menjayakan penyelidikan ini.

## CONTENTS

| CHAPTER   | TITLE  | PAGE |
|-----------|--|------|
|           | ACKNOWLEDGEMENT                                  | iv   |
|           | ABTRACT  | v    |
|           | ABSTRAK  | vi   |
|           | CONTENTS   | vii  |
|           | LIST OF FIGURE                                   | x    |
|           | LIST OF TABLE                                    | xii  |
|           | LIST OF APPENDICES                               | xiii |
| <br>      |  |      |
| CHAPTER 1 | INTRODUCTION                                     |      |
|           | 1.0 Background                                   | 1    |
|           | 1.1 Objective                                    | 2    |
|           | 1.2 Scope  | 3    |
|           | 1.3 Methodology                                  | 3    |
| <br>      |  |      |
| CHAPTER 2 | WAKE WASH STUDY                                  |      |
|           | 2.1 Wave Patterns                                | 5    |
|           | 2.2 Theory of wave formation and propagation     | 9    |
|           | 2.3 Definition of terms used in analysis         | 10   |
|           | 2.4 Prediction of Wash Wave Height               | 13   |
|           | 2.5 Factor influencing wave wake characteristics | 14   |
|           | 2.6 Ships wash                                   | 15   |
|           | 2.7 Wake wash impact                             |      |



|       |                                |    |
|-------|--------------------------------|----|
| 2.7.1 | Potential impact to shorelines | 16 |
| 2.7.2 | Potential impact to marinas    | 17 |
| 2.8   | Parameter those affect wake    | 18 |
| 2.9   | Design for minimum wake wash   | 18 |

### **CHAPTER 3                      WAKE WASH PHENOMENA**

|     |                           |    |
|-----|---------------------------|----|
| 3.1 | Technical Background      | 20 |
| 3.2 | Vessel generated waves    | 22 |
| 3.3 | Vessel wake wash patterns | 23 |
| 3.4 | Effect of water depth     | 28 |

### **CHAPTER 4                      DEVELOPMENT OF INSTRUMENTATION AND DATA ACQUISITION SYSTEM**

|       |  |    |
|-------|--|----|
| 4.1   | Water Wave Probe                           |    |
| 4.1.1 | Design requirement                         | 30 |
| 4.1.2 | Principal operation                        | 31 |
| 4.1.3 | Material selection for wire probe          | 31 |
| 4.1.4 | The wire probe specification               | 34 |
| 4.2   | Data Acquisition Systems and LabView       |    |
| 4.2.1 | Introduction                               | 35 |
| 4.2.2 | Computer Base Data Acquisition<br>Overview | 36 |
| 4.2.3 | Sampling                                   | 36 |
| 4.2.4 | ADC  | 38 |
| 4.2.5 | Resolution                                 | 38 |
| 4.2.6 | Data Transfers to the computer             | 39 |

|       |                  |    |
|-------|------------------|----|
| 4.2.7 | LabView Software | 41 |
|-------|------------------|----|

## **CHAPTER 5      EXPERIMENT IN SHALLOW WATER**

|     |  |    |
|-----|--|----|
| 5.1 | Instrumentation and Data Acquisition setup   | 45 |
| 5.2 | Test conditions and data presentation result | 49 |
| 5.3 | Model Preparation                            | 51 |
| 5.4 | Wave Probe Calibration Method                | 54 |
| 5.5 | Result and Discussion                        | 57 |

## **CHAPTER 6      CONCLUSION AND RECOMMENDATION**

|     |                |    |
|-----|----------------|----|
| 6.1 | Conclusion     | 72 |
| 6.2 | Recommendation | 73 |

|                   |  |           |
|-------------------|--|-----------|
| <b>REFERENCES</b> |  | <b>74</b> |
|-------------------|--|-----------|

## CHAPTER I

### INTRODUCTION

The wake wash generated by vessels has become an issue of international importance, especially for densely populated and active harbor areas. Some of the main concerns are <sup>[7]</sup> :

- Safety of passing vessels, particularly small craft
- Impact to vessels in exposed and partially-protected dock areas and marinas
- Safety of passengers unloading from other ships at harbor terminals
- Damage to bulkheads and other shoreline structures
- Erosion of natural shorelines and wetlands
- Biological impacts on offshore kelp beds and clam beds

The waves generated by high-speed craft are in general not very large compared to storm waves. However the high occurrence due to regular ship service over a long period of time can cause disturbance to marinas, shoreline and seabed, in particular in shelter bays, channels and sounds.

The aimed of this study is to investigate wake wash characteristic from patrol craft. From this investigation, it can be realize the full potential of high-speed craft in satisfying the urban transportation needs. This characteristic will be very importance when the operating zones happen to be in close proximity to shores/banks and other water users, as is the case most often in urban harbors, this poses potentially significant safety and environmental challenges.

## 1.1 Objective

The objective of this research is to study a wake wash characteristic from patrol craft and also to develop instrumentation and data acquisition for measuring wake wash.

## 1.2 Scope

The scope of this project is:

1. Literature study on wake wash characteristic.
2. Development of instrumentation and data acquisition using LabView to measure wake wash.
3. Wake wash measurement in towing tank.
4. Analyses of wake wash test result.

## 1.3 Methodology

First Part

1. Literature study on wake wash theory and pattern in different length and depth Froude Number.
2. Literature study on parameter those affect wake wash and how to minimize wash.
3. Material selection for wave probe.
4. Study on how water wave probe setup and operation.
5. Developments a procedure of wake wash measurement.

## Second Part

1. Literature study of LABVIEW
2. Literature study of Data Acquisition system
3. Development of instrumentation and data acquisition system using LabView to measure wake wash.
4. Water wave probe setup in towing tank.
5. Investigation of wake wash characteristic from patrol craft in towing tank
6. Analyses of wake wash test result.

## CHAPTER 2

### WAKE WASH STUDY

#### 2.1 Wave Patterns

In order to develop an appropriate measure it is first to review the principal characteristics of the well known wave pattern generated by a vessel in deep water. As a ship moves across the surface of a body of water, a wave pattern consisting of divergent and transverse wave is generated. Diverging waves are created at the bow and stern and will generally remain separated throughout their travel. Transverse waves, also created at the bow and stern will, however, combine to form a single series of waves. Kelvin (1887) found that, for any deep water speed, the diverging and transverse wave form a constant pattern and meet to form a locus of cusps whose angle with sailing line is  $19^{\circ} 28''$ . A typical Kelvin wave pattern is shown in figure 1. Kelvin's theory also predicts that the angle between the sailing line and the bow and stern diverging wave crest lines at the cusp locus line should remain constant at  $54^{\circ} 44''$ .<sup>[12]</sup>

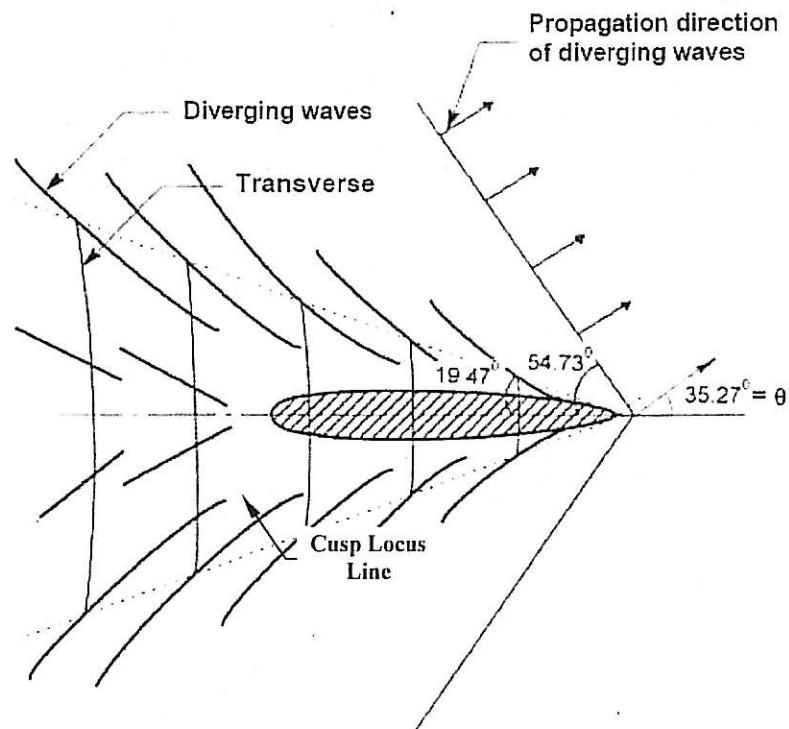


Figure 1: Kelvin wave pattern in deep water<sup>[13]</sup>

According to Kelvin's theory the celerity of the transverse waves ( $C_t$ ) is equal to the speed of the ship ( $V_s$ ), whereas the celerity of the diverging waves ( $C_d$ ) is equal to the ship speed projected onto the propagation direction of the diverging waves. That is, in deep water:

$$C_t = V_s$$

$$C_d = V_s \cos \theta$$

$$C = \frac{gT}{2\pi}$$

$\theta$  is the angle between the propagation direction of the diverging waves and the vessel course.  $c$  is the wave celerity (m/s) and  $T$  is the wave period (s). From the above expressions, the following relation between the wave period of the diverging waves, the

propagation direction of the diverging waves and the ship speed can be derived for deep water:

$$T = \frac{2\pi V_s \cos \theta}{g}$$

This simplifies to  $T \approx 0.27 V_s$ , and  $c \approx 0.42 V_s$ , respectively, where  $V_s$  states the ship's speed in knots. <sup>[13]</sup>

In water of medium to low depth, the ship-generated wave pattern will be different from the deepwater wave pattern. For depth-Froude numbers less than 1, the following empirical expression for the wave propagation direction of the diverging waves as a function of  $F_{nh}$ .

$$\theta = 35.267^\circ(1 - e^{12(F_{nh}^{-1})}) \quad \text{for } F_{nh} < 1 \quad (2.1.1)$$

(Consequently  $\theta$  will decrease from  $35^\circ 16'$  to zero degrees). <sup>[13]</sup>

For a Froude number larger than 1, the transverse waves disappear and the diverging waves remain. The wave propagation direction increases for increasing Froude numbers, the angle between the wave fronts and the navigation track decreases.

Contrary to the Kelvin type wake wash, the wave period and wave propagation direction for the diverging waves cannot only be estimated from the speed of the ship. This is because the wave celerity in finite water depth is depending on the water depth.

However, in shallow water where  $\frac{h}{L} < 0.05$  ( $h$  being the water depth and  $L$  the wavelength), the expression for the wave propagation direction becomes particularly simple, that is: <sup>[13]</sup>



$$c = \sqrt{gh} = V_s \cos \theta$$

$$\frac{\sqrt{gh}}{V_s} = \cos \theta$$

$$\frac{1}{F_{nh}} = \cos \theta$$

$$\theta = \cos^{-1} \frac{1}{F_{nh}} \quad \text{for } F_{nh} > 1$$

(2.1.2)

The relationship between the wave propagation direction and the depth Froude number depicted in Figure 2 below.

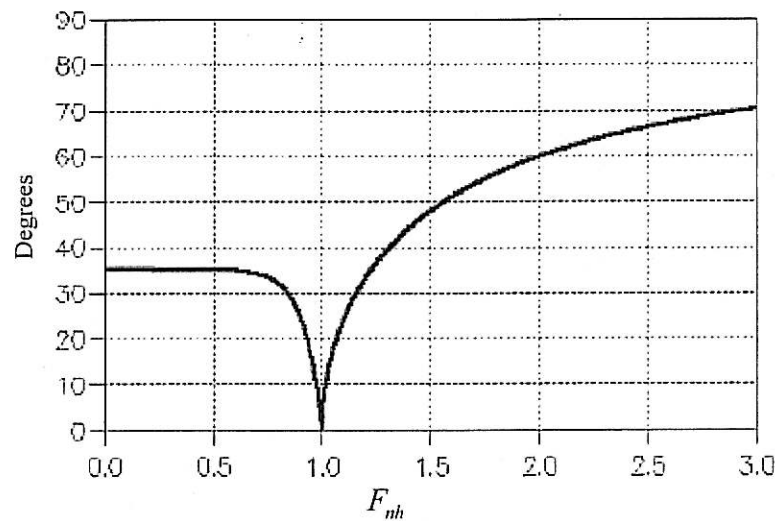


Figure 2: Wave propagation direction for diverging waves versus the depth-based Froude number.

## 2.2 Theory of wave formation and propagation.

Most waves that observe in the ocean are wind generated waves and wind generated waves are often confused by several factors such as fluid motion beneath the wave surface and the confusion of several sets of wave patterns merging. However a simple wind generated wave is similar in format to a vessel generated wave that has traveled a distance from the vessel. These waves eventually assume a sinusoidal or simple harmonic form and can be analyzed with classic sinusoidal theory. The terms and measurable criteria are illustrated in Figure 3.

Without significant interference from other wave systems, a vessel generated wave that has traveled a few ship lengths from the point of generation will assume a form so close to that of the sinusoidal wave, that can use classic wave theory to quantify and characterize the wash generated by various hull forms and specific vessels. This wave theory is defined by the following basic characteristics, illustrated in Figure 3.

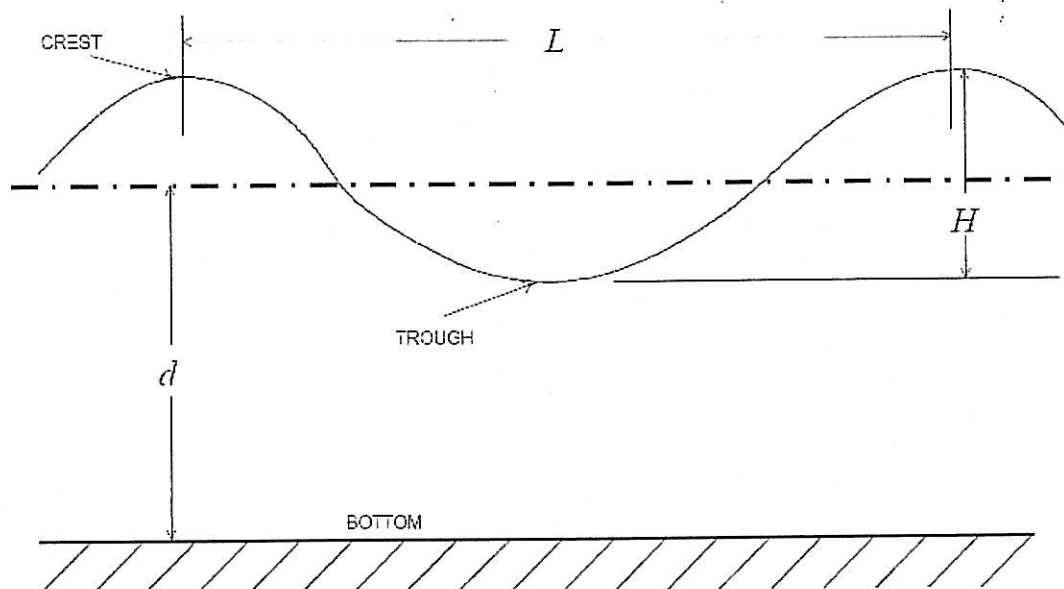


Figure 3: Basic Wave Characteristics<sup>[5]</sup>

- L The length of the wave from one point to the same point on the next wave.
- H The height of the wave from crest to trough
- T The time that it takes for two successive wave crests to pass a given point.
- Although we often note steeper and sharper waves closer to the line of travel of the vessel, if we get several vessel lengths away, the sinusoidal theory gives us a good basis for comparison of waves characteristics between various vessels.

### 2.3 Definition of terms used in analysis.

**Wake Wash Height:** the height, measured in centimeters, from peak to trough, of the highest wave in the series of waves produced by the passing of the measured vessel. Wake wash height is measured or mathematically normalized to a distance of 300meters perpendicular to the centerline of travel of the vessel. 300 meters is chosen to provide a basis for comparison between various vessels measured under similar circumstances by the investigators. <sup>[6]</sup>

**Wake Wash Period:** the time, in seconds, for one complete wave cycle to pass a fixed point. The period of the highest wave in the series of waves produced by the passing of the measured vessel is determined by the time difference between the zero crossing of the start of the highest wave and the zero crossing of the start of the next wave in the series. <sup>[6]</sup>

**Wash Energy:** The relative damage to the beach, to a passing vessel, or to a shore structure is a function of the amount of energy expended by the wave front upon impact. This function is not easily measured directly but have the measurable quantities from which energy density per linear meter of wave front can be calculated show below. <sup>[6]</sup>

The energy is the sum of the potential and kinetic energy and is given by:

$$E = E_{kinetik} + E_{potential}$$

$$E = \frac{\gamma g H^2 L}{16} + \frac{\gamma g H^2 L}{16}$$

$$E = \frac{\gamma g H^2 L}{8}$$

where  $\gamma$  is the density of water,

$g$  is the acceleration due to gravity,

$H$  is the wash height,

$L$  is the wash wavelength.

The term for wavelength in this formula is to be replaced by a function of wash period from the relationship given below:

$$L = \frac{gT^2}{2\pi} \quad \text{in deep water.}$$

resulting in the following equation:

$$E = \frac{\gamma g^2 H^2 T^2}{16\pi}$$

In metric units, with  $H$  in meters and  $T$  in seconds, this formula reduces to:

$$E = 1961H^2T^2$$

with energy density expressed in joules per meter of wave front.

A few parameters are used to describe the wave traces and patterns. They are as follows and are illustrated in figure 4.

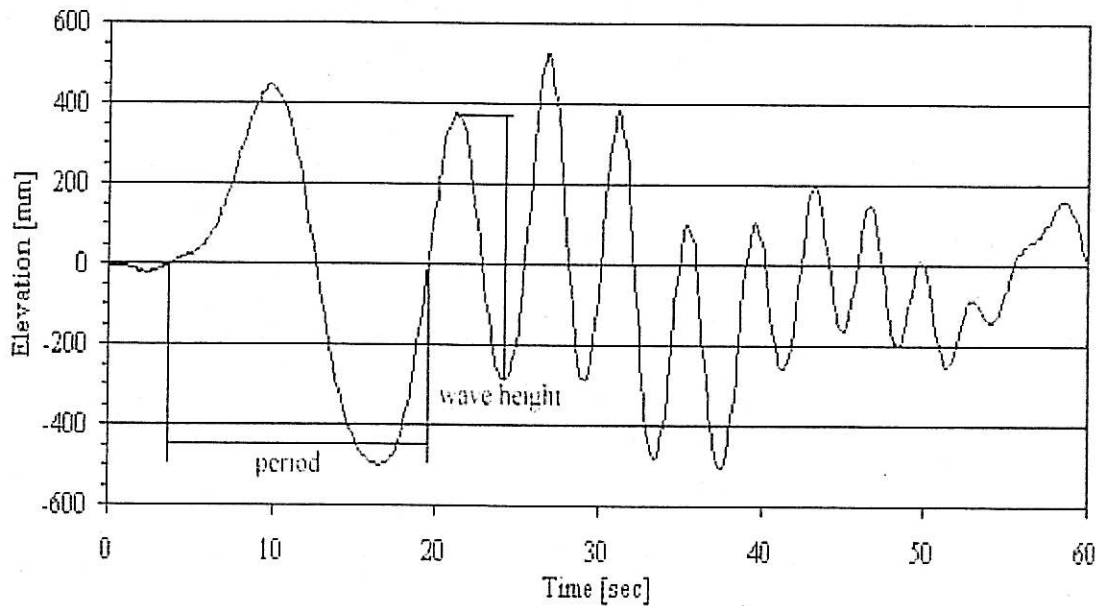


Figure 4: Wave Elevation Time History<sup>[9]</sup>

- H - is the wave height, measured from a crest to the next trough after a zero crossing. The maximum wave height  $H_{\max}$  is the highest wave measured in a trace.
- T - is period, measured from one upward zero crossing to the next positive zero crossing. The maximum period  $T_{\max}$  is the period of the highest wave.

#### 2.4 Prediction of Wash Wave Height

The values of ship generated wave heights were predicted using a recently published regression model produced by Kriebel, Seelig, and Judge (2001). The equations are developed from regression analyses of data collected by the authors with

adjustments to satisfy some theoretical considerations. The model also is based upon a regression analysis of ship generated wave data from model tests of a wide variety of vessels include patrol craft.

The formulas they provide are mostly a modification and combination of those produced by Sorensen and Weggel, (1986) and Gates and Herbich (1977). The vessels in the data set were only tested at  $F_{nh}$  up to 0.8, with most of the data points in the 0.3 to 0.8 range. So formulas are only relevant for  $F_{nh}$  up to 0.8, and that predictions below  $F_{nh}$  of 0.3 will be less accurate.

Table 1: The formulas proposed by Kriebel, Seelig, and Judge (2001) are as follows<sup>[8]</sup>

|  |   |
|--|---|
| $\frac{gH}{V_s^2} = \beta(F_* - 0.1)^2 \left( \frac{y}{L} \right)^{-\frac{1}{3}}$ $H = \frac{V_s^2}{g} \beta(F_* - 0.1)^2 \left( \frac{y}{L} \right)^{-\frac{1}{3}}$ | Height of the largest wave in the wave train at a distance y from the sailing line of the vessel. |
| $F_* = F_d (e)^{\frac{R}{d}}$  | Modified depth Froude number that accounts for vessel length and draft and form.                  |
| $\alpha = 2.35(1 - C_b)$   | A parameter related to hull form – mostly the block coefficient.                                  |
| $\beta = 1 + 8 \tanh^2 \left( 0.45 \left( \frac{L}{Le} - 2 \right) \right)$  | A parameter related to hull form – mostly the bow angle   |

H... Maximum ship generated wave height, m

C... Celerity, m/s (wave speed)

$F_L$ ... Length based Froude number

$F_d$ ... Depth based Froude number

$F_*$ ... Modified depth based Froude number

$L_{BP}$ ... Ship length between perpendiculars, m

d... Water depth, m

- R... Ship draft, m  
 C<sub>b</sub>... Ship block coefficient  
 L<sub>e</sub>... Bow entrance length, m  
 V<sub>s</sub>... Ship Speed, m/s  
 α... Coefficient related to hull form – Used in wave height regression analysis  
 β... Coefficient related to bow shape – Used in wave height regression analysis  
 y..... Distance from sailing line, m  
 L<sub>w</sub>... Wavelength, m  
 θ... Angle between sailing line and line perpendicular to direction of diverging waves

## 2.5 Factor influencing wave wake characteristics

Many factors contribute to an individual wave wake pattern making a complete study very complex. The major factors can be considered as either vessel related, environment related or other: <sup>[12]</sup>

| <i>Vessel related:</i> | <i>Environment related:</i> | <i>Other:</i>                  |
|------------------------|-----------------------------|--------------------------------|
| - speed                | - water depth               | - distance from sailing line   |
| - direction            | - tide level                | - wake interactions            |
| - hull form            | - tidal stream direction    | - location of measurement site |
| - draft                | - tidal stream velocity     |                                |
| - loading              | - coastal morphology        |                                |
| - trim                 | - wind wave characteristics |                                |
|                        | - sub-surface flows         |                                |

## 2.6 Ships Wash

Ships generate waves, which get bigger and more energetic the faster the ship goes relative to its length. The magnitude of the waves generated by a vessel are related to the following variables: <sup>[10]</sup>

- the speed of the vessel (as the speed of the vessel increases, the waves generally increase in size),
- the size and displacement of the vessel, and
- the distance between the vessel and the marine feature of interest (clearly the wave energy at the foreshore and hence the potential for erosion will be dependent upon the distance from the source of the wash, the form of the seabed and any other obstacles).

The energy in the waves is a function of speed and displacement. Therefore, the generation of ships' wash will be highly specific to the type and design of vessel, and it cannot be assumed that the larger or faster a vessel the greater the wash generated as this is not always the case. The wave energy generated by moving vessels should be considered in relation to the background wave climate in an area. <sup>[10]</sup>

Examples of how vessel type can affect wash include the following considerations: <sup>[10]</sup>

- Small fast power cruisers proceeding just 'off the plane' will make more wash than if they were in a fully planing mode at maximum speeds.
- High speed hulls, such as planing hulls or narrow low-wash catamaran hulls may produce little wash.
- Hovercraft makes a depression in the water under the cushion which can have poor wash characteristics.



## 2.7 Wake wash impact

### 2.7.1 *Potential Impacts to Shorelines*

New routes and increased frequency of ship across the Bay could increase the wave height (energy) at some shorelines, potentially causing increased erosion.

Shorelines tend to be in dynamic equilibrium with the “typical” or average wind wave energy reaching them. Erosion could be increased or altered due to additional ship moving if wake wave heights and energy were significantly greater than those of existing wind-driven waves.

For shorelines at a distance greater than 1,500 meters\* from a proposed ship moving, impacts are not anticipated to be significant. Impacts could potentially be significant for sensitive shorelines (tidal marshes and mudflats) that are within 1,500 meters\* of a ship route. Impacts are not anticipated at rocky or armored shorelines as these shorelines can withstand extreme weather events, which subject them to conditions only experienced every 50 or 100 years.

\* The 1,500-meter criterion is based on distance required for the wake from a vessel’s design wake wave height of 27 cm (measured at 300 meters) to attenuate to the 16 cm shoreline criterion.

### **2.7.2 *Potential Impacts to Marinas***

Increased frequency of ship moving across the bay could increase the wave heights at surrounding marinas, potentially damaging moored vessels and interfering with recreational users.

Individual wave height is the primary factor of concern for impacts at unprotected marinas, due to the potential for damage of moored vessels, docks, etc., or potential safety issues for users of the marina.

### **2.8 *Parameter those affect wake***

Wake characteristics vary not only as a function of the vessel's speed, trim, and direction of travel, but also as a function of hull characteristics. Hull designs that more easily achieve high-speed planning are far more energy efficient and generate far lower wake energy than less efficient hull designs. Clearly, hull designs that minimize wake production are desirable from both an adverse impacts standpoint and an operational standpoint.<sup>[13]</sup>

### **2.9 *Design for minimum wake wash***

A design goal of low wake wash can be achieved by designing a vessel that achieves hump speed as early as possible and with the lowest possible hump wash height and energy density. Hump speed (for wake wash) increases with waterline length. Therefore, minimizing waterline length in a given design will reduce the hump speed. However, short waterline lengths may increase pitching and increased bow flare above the waterline may be required.

In general, wash height and energy density at hump speed are inversely proportional to length-to beam ratio ( $LWL/B$ ). Also, high  $LWL/B$  seems to contribute to getting through the hump more rapidly. Therefore, reduction of waterline length without reduction of the beam will decrease the length-to-beam ratio and minimizing the hump in both height and energy density depends on the highest possible length-to-beam ratio. So, to maintain length-to-beam ratio as the waterline length is reduced, the beam must also be reduced. The only way, then to maintain displacement is to increase draft as conceptually illustrated in Figure 5.

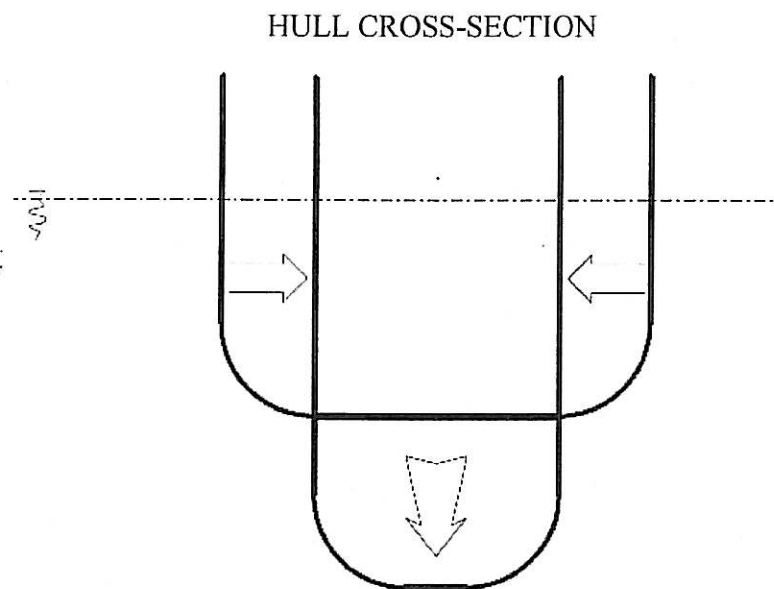


Figure 5: Reducing hull beam and increasing draft<sup>[5]</sup>

Increasing draft to maintain displacement will increase the wetted surface of the vessel and therefore, may significantly raise the powering requirements for a given service speed. If wake wash is the paramount criteria or a very important one, the added power and fuel consumption may be a price worth paying.<sup>[5]</sup>

## CHAPTER 3

### WAKE WASH PHENOMENA

#### 3.1 Technical Background

A vessel of common hull shape traveling through still water will experience <sup>[8]</sup>

- a pressure rise in the bow vicinity;
- pressure drop below the free stream pressure over the midsection; and
- a pressure rise again at the stern.

The water surface responds to this pressure gradient by rising at the bow and stern and falling along the midsection. Pressure gradient and water surface rise at the stern is usually less than that at the bow because of flow separation at the rear section of the hull.

The sharp pressure gradient at the bow and possibly at the stern induce a rapid rise and fall in the water surface but inertia causes the water surface to lag behind its equilibrium position and produces a surface oscillation. This in turn produces two (or more) sets of patterns of free waves that propagate out from the vessel, one at the bow and one at the stern. Sometimes, wave systems are generated at other high pressure areas such as the bow shoulders. Normally however these waves are so small they can be disregarded. The set of waves developed from the stern is also usually much smaller than those from the bow and are generally not considered. Each system of waves (at low speeds) will consist of transverse waves moving in the same direction as the vessel, and divergent waves moving obliquely away from the vessel. This is the classic Kelvin wave system. At high speeds, and/or low water depth only a divergent wave system is produced.

The height of the resulting ship generated waves depend on the magnitude and distribution of the pressure gradient which in turn depends upon the vessel speed, hull surface geometry, draft, trim, and where applicable the depth of the water and channel cross section shape. The period and direction of propagation of the vessel generated waves depend only on the vessel speed and water depth. As the waves propagate away from the vessel, in constant depth water, dispersion will cause the wavelength to increase and the wave height to decrease, with an overall reduction in energy level. The distance from the sailing line is thus important for assessing the energy in the wake wash at that location.

A very brief overview of wake wash theory applicable to the current study will present in this thesis. The formula and methodology used to predict wake wash are also presented.

### 3.2 Vessel Generated Wash

With few exceptions (and those are weird shapes), every vessel moving through the water generates two sets of waves, *divergent waves* which move out at an angle from the centerline of travel and *transverse waves* (Kelvin wake), which move out from the stern perpendicular to the centerline of travel. These are easily noticed when viewed from above in an airplane or from a bridge as a vessel passes beneath. They are illustrated in Figure 6.

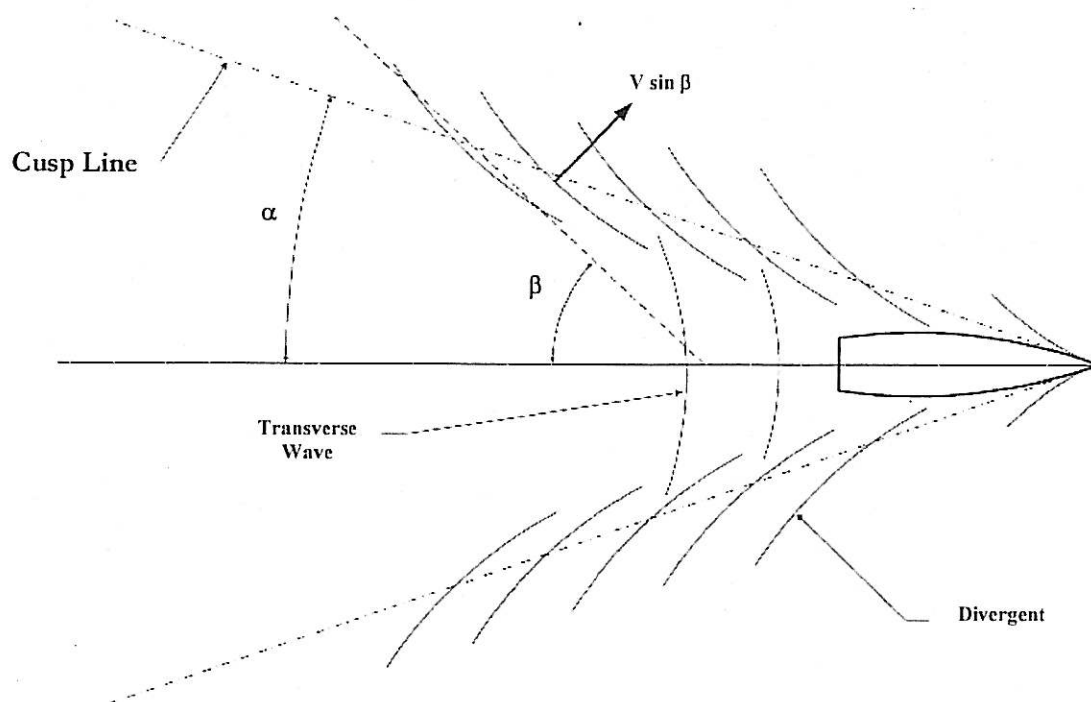


Figure 6: Vessel Generated Waves<sup>[2]</sup>

The generation of the divergent waves is a function of hull form (Prismatic coefficient), angle of entry, speed, and speed-length ratio  $V/(L_s)^{0.5}$  and is significant in the development of the height and energy of the wave train, particularly at low or intermediate speeds. The transverse wave form is usually negligible at low speeds but increases with speed up to a length Froude Number of about 0.6 and at higher speeds the transverse wave disappears in the range of  $0.6 \leq F_n \leq 1.0$  leaving a bow divergent wave and a stern divergent wave.

The angle  $\alpha$  in salt water develops to be  $19.46^\circ$  initially for all ships but the angle of obliquity  $\beta$ , varies with hull form and speed, being lower at higher speed length ratios ( $4^\circ$ - $10^\circ$ ) and higher for lower speed length ratios and fuller hull forms ( $20^\circ$ - $30^\circ$ ).

The significance of the angle of obliquity ( $\beta$ ), is that the direction of the movement of the energy front will be as shown in figure 6 and the wave length ( $L$ ) and wave period ( $T$ ) will be affected by the angle of wave generation. In general, the finer

the bow entry, the smaller the angle  $\beta$  and thus the smaller the wavelength and period. This smaller wavelength results in a lower energy density for a vessel's wash. [2]

### 3.3 Vessel wake wash patterns.

The best measure of deep water for vessel generated waves is the Depth Froude Number, given by: [4]

$$F_{nh} = \frac{V}{\sqrt{gh}} \quad , \text{where } V \text{ is vessel speed,}$$

$g$  is the gravitational constant,

$h$  is the water depth

For the purpose of wash comparison, vessels may be considered to be free of shallow water effects when  $h/L_{WL}$  exceeds 1.

The Depth Froude Number is critical in determining wash characteristics in shallow water, just as the Length Froude Number is in determining wash characteristics in deep water. However, the influence of the critical value of  $F_{nh}$  is much more visible, dramatic and well defined than that of the Length Froude Number. The Length Froude Number is given by: [4]

$$F_{nl} = \frac{V}{\sqrt{g(LWL)}}$$

The main categories are as follows;

- sub-critical  $F_{nh} < 1$
- critical ship speed = maximum wave speed  $F_{nh} = 1$
- super-critical ship speed > maximum wave speed  $F_{nh} > 1$
- high speed sub-critical similar to sub-critical but recognises that high speed ships in deep water can produce divergence waves with or without the transverse wave component depending on the length Froude number (the ratio of ship velocity to a function of waterline length),
- trans-critical or near-critical depth Froude numbers between 0.85 and 1.1.

Below the critical value of  $F_{nh} = 1.0$  the wash pattern for a vessel with a  $F_{nl}$  less than about 0.9 appears as shown in Figure 7.

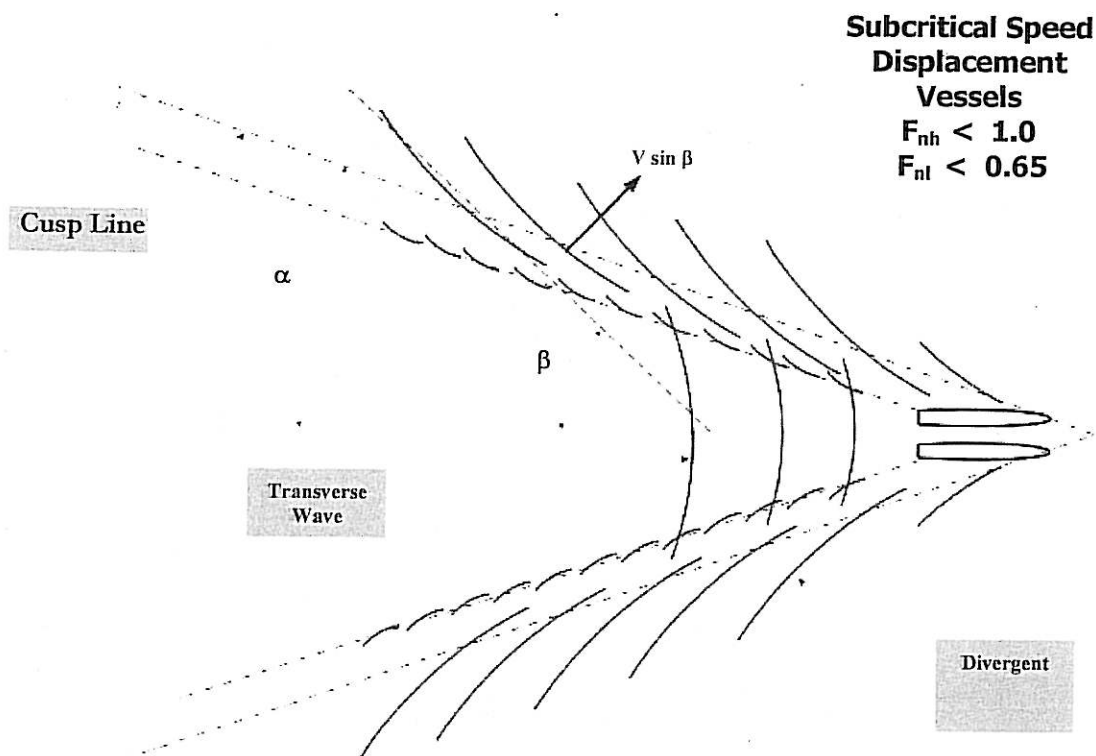


Figure 7: Sub-critical wash pattern for displacement vessels<sup>[4]</sup>



If a vessel is transiting from deep water to shallow water at constant speed, at  $F_{nl}$  values less than about 0.9, and we cross this critical depth in relation to that speed, the direction of wave propagation will be seen to change from that shown in Figure 7 to the pattern shown in Figure 8.

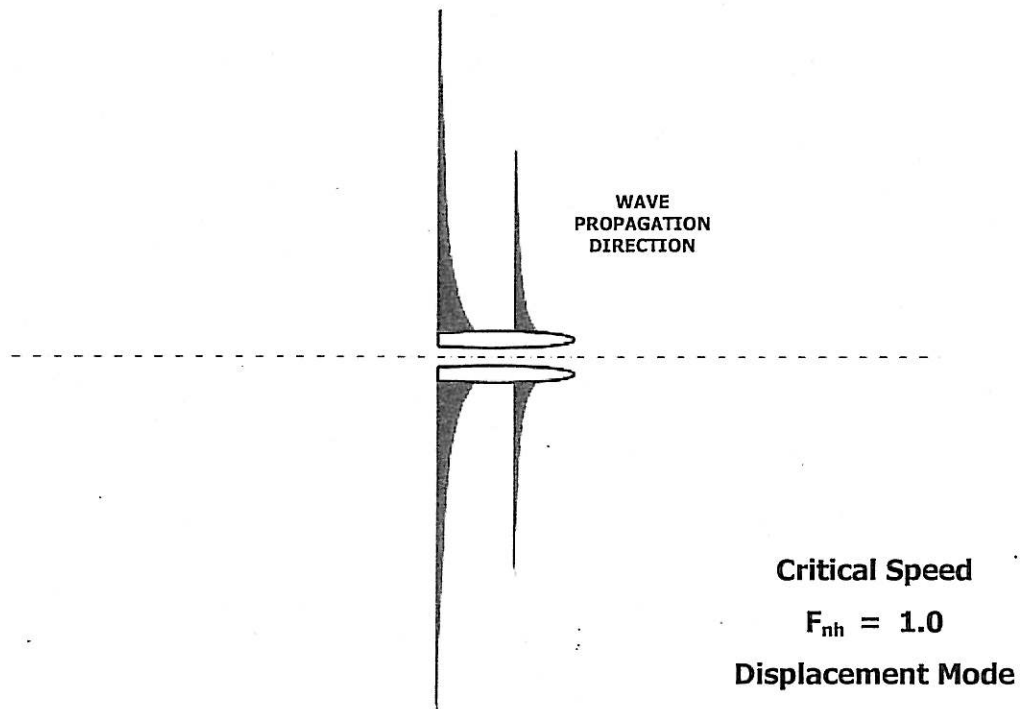


Figure 8: Critical wash pattern for displacement vessels<sup>[4]</sup>

For vessels with a value of  $F_{nl}$  approaching and exceeding 1.0, the wash pattern will be the standard pattern depicted in Figure 9, and will not produce the critical wave shown in Figure 8.

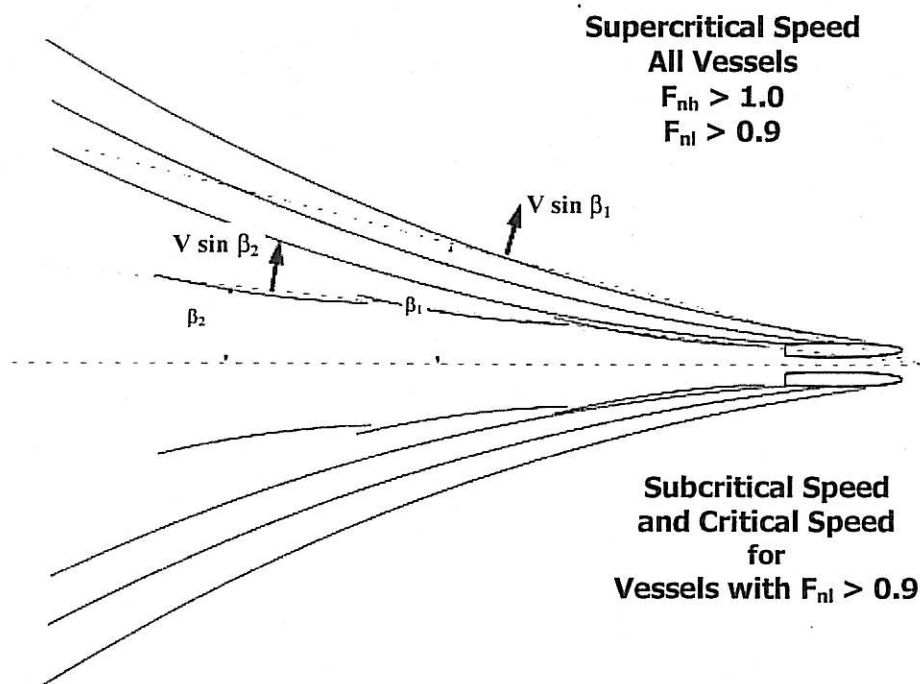


Figure 9: Wash pattern for supercritical operation and all vessels at speeds above  $F_{nl} = 0.9$ <sup>[4]</sup>

For vessels that are somewhere below  $F_{nl} \approx 0.9$  but not in the region below the hump ( $F_{nl} < \sim 0.65$ ), the wash pattern will be somewhere between the two conditions of Figure 9 and Figure 7. All of this can be quite important in predicting the character of the wash and where it will reach a given beach.

### 3.4 Effect of Water Depth

In shallow water, the pressure gradient on the hull, and therefore the wave pattern generated by the vessel is influenced by the waves reflecting from the sea bottom. When a wave is propagating in water having a depth of less than approximately

half the length of the wave, the wave induced water particle motion reaches the bottom and the water depth affects wave characteristics.

In shallow water the wave speed (celerity) of a gravity wave is given by

$$C = \frac{L}{T} = \sqrt{gd}$$

The ratio of the vessel speed to the maximum wave celerity in shallow water is often used to classify the wash produced by a vessel. This ratio, called the Depth Froude Number is defined as follows.

$$F_{nh} = \frac{V}{\sqrt{gh}}$$

At  $F_{nh} = 1$ , the wave speed has increased to its physical maximum of  $\sqrt{gd}$ . Normally the transverse wave will travel at the same speed as the vessel, however since it physically can't go any faster, the wave gets much larger, and the ship resistance increases dramatically.

In deep water the vessel length Froude number,

$$F_{nl} = \frac{V}{\sqrt{g(LWL)}}$$

is used to classify wash. At a critical value of  $F_{nl} \sim 0.4$  to  $0.55$  the wavelength of the transverse waves equals the ship length giving a condition similar to the critical condition in shallow water.

For most displacement vessels, in normal speed ranges, there is no strong wave bottom interaction if the water depth to draft ratio,  $d/T$ , is greater than 3 to 5. The  $d/T$

ratio will most often be less than 3 for the displacement vessels being studied, thus  $F_{nh}$  has been used in analysis.

Vessel generated wake wash in shallow water is usually classed in three categories. Those produced by vessels that travel at sub critical Froude numbers, those produced at the critical Froude number of 1, and those produced by vessels that operate at supercritical Froude numbers such as planing craft and multi hulls. Normally the cruise ship operates at sub critical Froude numbers whereas the patrol vessel generally operates at supercritical speeds and is treated separately.

## CHAPTER 4

### DEVELOPMENT OF INSTRUMENTATION AND DATA ACQUISITION

#### 4.1 Water Wave Probe

##### 4.1.1 Design Requirement

The requirements of any measuring instrument are: firstly, that the sensing element must not affect the entity being measured, except perhaps to a negligible degree; secondly, that the instrument output be a convenient function of the entity being measured, and if it depends on other factors, these must not vary; and thirdly, the instrument must be readily used and not unnecessarily complicated.



##### 4.1.2 Principal Operation

The method is free of meniscus and 'wetting' effects. It operates on the principle of measuring the current flowing in an immersed probe that consists of a pair of parallel wire. The current flowing between the probe wires is proportional to the depth of immersion and this current is converted into an output voltage proportional to the instantaneous depth of immersion. The output circuitry is suitable for driving both a chart recorder and data logger.

### 4.1.3 Material Selection

Table 2: Conductivity of common materials

| Material             | IACS  | (Conductivity)<br>MSm <sup>-1</sup> |
|----------------------|-------|-------------------------------------|
| Silver (pure)        | 107   | 62                                  |
| Copper Annealed      | 100   | 58                                  |
| Gold                 | 78    | 45                                  |
| Aluminium (pure)     | 65    | 38                                  |
| Brass (Cu-Zn) 5% Zn  | 55    | 32                                  |
| Aluminium Alloys     | 25-60 | 15-35                               |
| Magnesium            | 39    | 23                                  |
| Brass (Cu-Zn) 15% Zn | 37    | 21                                  |
| Molybdenum           | 33    | 19                                  |
| Al 7075-76           | 32    | 18.5                                |
| Tungsten             | 32    | 18.5                                |
| Al 2024-74           | 30    | 17.5                                |
| Zinc                 | 29    | 17                                  |
| Brass (Cu-Zn) 30% Zn | 28    | 16                                  |
| Brass + Lead         | 12-25 | 7-14.5                              |
| Magnesium Bronze     | 24    | 14                                  |
| Beryllium Copper     | 24    | 14                                  |
| Cu/Ni (90/10)        | 12    | 7                                   |
| Lead                 | 8     | 4.5                                 |
| Cu/Ni (70/30)        | 5     | 3                                   |
| Zirconium            | 4     | 2.5                                 |
| Stainless Steel      | 2.5   | 1.5                                 |
| Titanium             | 1-4   | 0.5-2.5                             |
| Inconel 600          | 1     | 0.58                                |


  
*Anodic*
  

  
*More Noble*
  
*Cathodic*

$$\%IASC = Msiemens\ m^{-1} \times 0.58$$

$$Msiemens\ m^{-1} = \%IASC \times 1.724$$

Drinking water: 0.005 – 0.05 S/m (50-500  $\mu$ S/cm). The conductivity of water changes with temperature (2% per  $^{\circ}$ C approximation) and it is also dependent on the concentration of dissolved salt in the hydraulic model.

Aims of this study are to select a useful material that can give higher sensitivity probe application. Higher sensitivities are achievable by using thinner, higher resistance elements but this significantly reduces the life of the probe. [11]

$$R = \rho \times \frac{L}{A}$$

where        R = resistance  
                   ρ = resistivity (Ohm.m)  
                   L = length (m)  
                   A = cross section area (m<sup>2</sup>)

|  |
|--|
| Resistivity (Ohm.m) , $\rho = \frac{1}{\text{conductivity}(\text{siemens})}$ |
|--|

Formula above showed relationship between resistance and resistivity. It can be conclude that, for higher resistance achieved by using lower conductivity material.

Material used also can avoid rapid corrosion because corrosion will affect the probe sensitivity and linearity measurement. It can be achieve by using a lower positioning material in galvanic series. All the specification needed discuss above can be achieve by using stainless steel for probe application.

Refer to the conductivity of common materials above, stainless steel will give a great material for probe application. With position more noble cathodic in galvanic series, this material can prevent and reduce electrolysis to a minimum value. Electrolysis will occur when different voltage applied to the probe.

#### 4.1.4 The wire probe specification

The size, shape and spacing of the wires is not critical thus enabling users to construct probes easily for special applications. The standard form of probe supplied consists of a pair of stainless steel wire:

1. Material: Stainless Steel wire
2. Diameter 0.5mm
3. Length 300mm
4. Wire spaced 12.5mm apart. (No great accuracy is required in the wire spacing and provided the instrument is properly setup, it is only necessary to ensure that gross distortion of the probe is avoided)
5. Cable length: Apply with 2m cable length. (Maximum resistance of 10 ohm per lag should consider)
6. Voltage output:  $\pm 3.18$  Volt maximum. (center zero)

## 4.2 Data Acquisition Systems and LabVIEW

### 4.2.1 Introduction

The DAQ card (made by National Instruments) are multi function plug-n-play, analog and digital input/output boards consisting of a onboard timer, 12 bit analog to digital converter (ADC) successive-approximation ADC with 16 single-ended or 8 differential analog inputs, 8 lines of TTL-compatible digital input, and 8 lines of digital output. The card also contains two 16-bit counter/timer channels for timing I/O. The optional 50 pin I/O connector for the card enables to easily connect all analog, digital, and timing signals directly to the card. The card is fully software configurable and



calibrated so that card will be install easily and begin acquisition without having to spend time configuring or calibrating the card.

Since the system is integrated with National Instruments products, it offers direct control of all hardware on the DAQ card from the LabVIEW software. LabVIEW is the emerging standard in visual programming based instrumentation control systems. LabVIEW is programmed with a set of graphical icons (called "G") which are connected with "wires". The combination of a DAQ card and LabVIEW software makes a virtual instrument or a vi. A vi can perform like an instrument and is programmable by the software with the advantage of flexibility of logging the data that is being measured.

#### **4.2.2 Computer based Data Acquisition Overview**

Traditionally, measurements are done on stand alone instruments of various types-oscilloscopes, multi meters, counters etc. However, the need to record the measurements and process the collected data for visualization has become increasingly important.

There are several ways in which the data can be exchanged between instruments and a computer. Many instruments have a serial port which can exchange data to and from a computer or another instrument. Use of GPIB interface board (General purpose Instrumentation Bus) allows instruments to transfer data in a parallel format and gives each instrument an identity among a network of instruments. All HP instruments in the EE Undergraduate Laboratories and PCs are equipped with GPIB interfaces.

Another way to measure signals and transfer the data into a computer is by using a Data Acquisition board. A typical commercial DAQ card contains ADC and DAC that allows input and output of analog and digital signals in addition to digital input/output channels.

### 4.2.3 Sampling

The data is acquired by an ADC using a process called sampling. Sampling a analog signal involves taking a sample of the signal at discrete times. This rate at which the signal is sampled is known as sampling frequency. The process of sampling generates values of signal at time interval as shown in following figure.

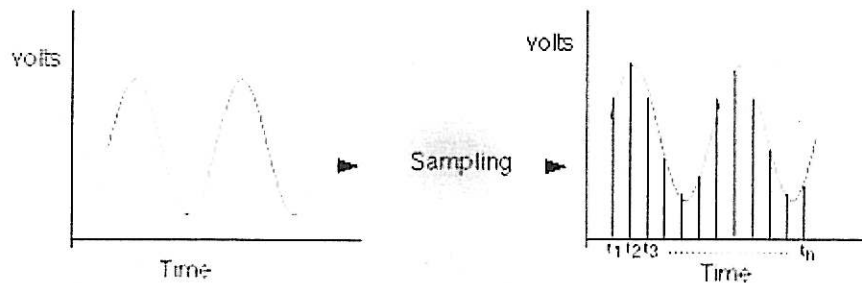


Figure 10 : Sampling process

The sampling frequency determines the quality of the analog signal that is converted. Higher sampling frequency achieves better conversion of the analog signals. The minimum sampling frequency required to represent the signal should at least be twice the maximum frequency of the analog signal under test (this is called the Nyquist rate). In the following figure an example of sampling is shown. If the sampling frequency is equal or less than twice the frequency of the input signal, a signal of lower frequency is generated from such a process (this is called aliasing).

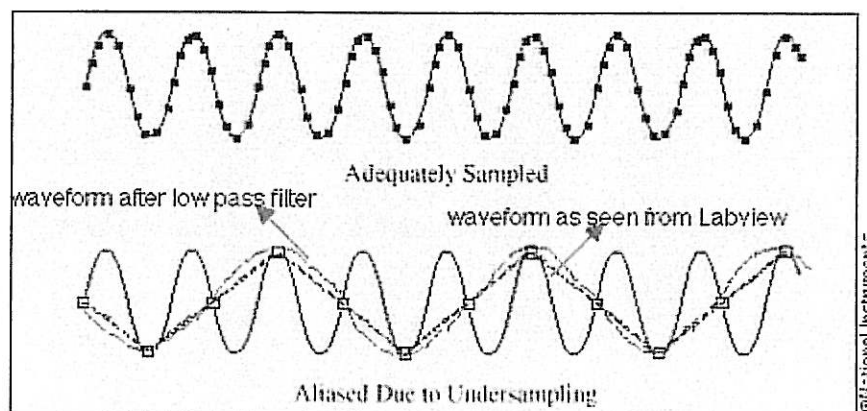


Figure 11: Effects of Sampling and aliasing due to undersampling

#### 4.2.4 ADC

Once the signal has been sampled, one needs to convert the analog samples into a digital code. This process is called analog to digital conversion. This is shown in Figure 12.

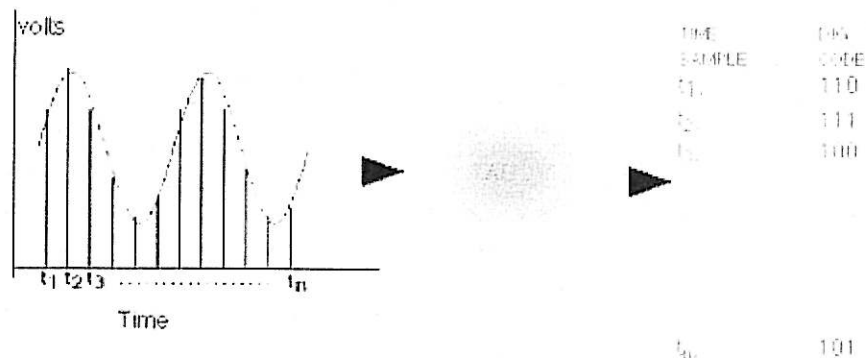


Figure 12 : Analog to Digital Conversion for a 3-bit ADC

#### 4.2.5 Resolution

Precision of the analog input signal converted into digital format is dependent upon the number of bits the ADC uses. The resolution of the converted signal is a function of the number of bits the ADC uses to represent the digital data. The higher the resolution, the higher the number of divisions the voltage range is broken into, and therefore, the smaller the detectable voltage changes. A 8 bit ADC gives 256 levels ( $2^8$ ) compared to a 12 bit ADC that has 4096 levels ( $2^{12}$ ). Hence, 12 bit ADC will be able to detect smaller increments of the input signals than a 8 bit ADC. LSB or least significant bit is defined as the minimum increment of the voltage that a ADC can convert. Hence, LSB varies with the operating input voltage range of the ADC. Figure 13 illustrates the resolution for a 3 bit ADC. FS stands for full scale and LSB is the least significant bit. If the full scale of the input signal is 10V then the LSB for a 3-bit ADC corresponds to  $10/2^3=1.25V$ . For a 12 bit ADC the least significant bit will be  $10/2^{12}=10/4096=2.44mV$ . If one needs to detect smaller changes, one has to use a higher resolution ADC. Clearly, the resolution is an important characteristic of the DAQ board.

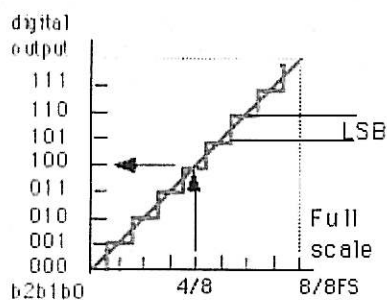


Figure 13: Resolution of ADC, X axis is analog input

#### 4.2.6 Data Transfers to the computer

Typically, DAQ card are installed in a PC with high speed data bus like PCI. Depending on the speed of the motherboard of the PC, the maximum data transfers can occur between microprocessor and memory at 20 MHz to 40 MHz. To improve the data transfers, bus mastering (allowing DAQ card to transfer data directly) is implemented as shown below in figure 14 and 15.

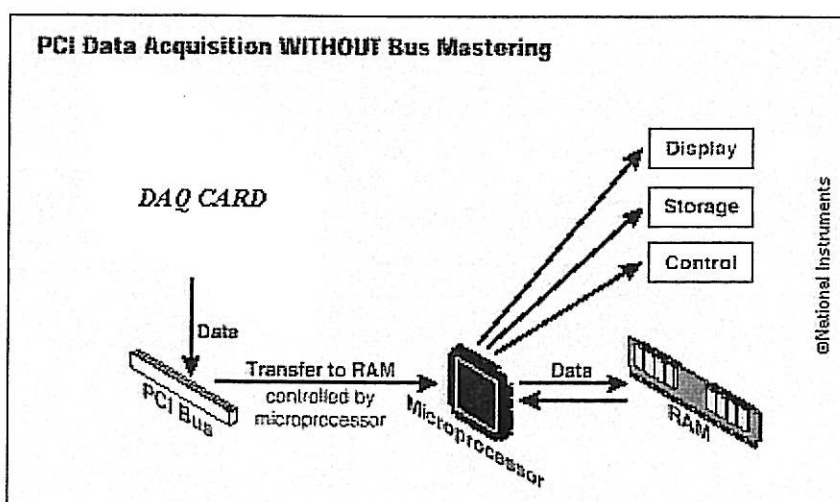


Figure 14: Data transfer without bus mastering (conventional)

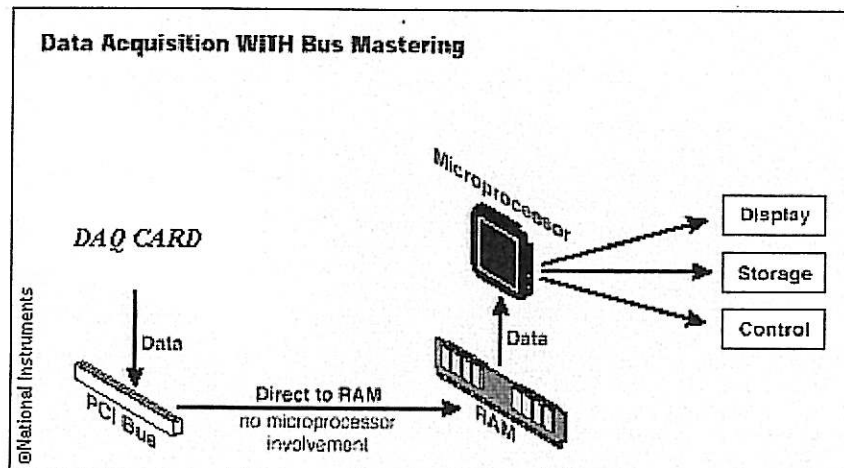


Figure 15: Data transfer with bus mastering (used in expensive DAQ boards)

#### 4.2.7 LabVIEW Software

DAQ hardware without software is of little use-and without proper controls the hardware can be very difficult to program. The purpose of having a appropriate software is the following:

- Acquire data at specified sampling rate
- Acquire data in the background while processing in foreground
- Stream data to and from disk

The driver software is a lower level driver that interfaces LabVIEW software with the DAQ card. As a user of LabVIEW one does not have to worry about configuration and control of components within DAQ card. LabVIEW identifies each board by a device number and therefore one can have as many devices as many as the computer can accept on their expansion slots. LabVIEW can also combine and display inputs from various sources like inputs from serial and parallel port, data acquisition card and GPIB card on a single interface.

LabVIEW is programmed with set of icons that represents controls and functions, available in the menu of the software. Such a programming is called visual programming and National Instruments calls it *G*. The user interface which is called a *vi* consists of two parts, a front panel and a diagram. This is similar to that of an instrument where a front panel is used for a input, output controls, and to display the data whereas the circuit resides on the circuit board. Similarly it can bring the buttons, indicators and graphing and display functions on the front panel as shown in figure 16 and figure 17.

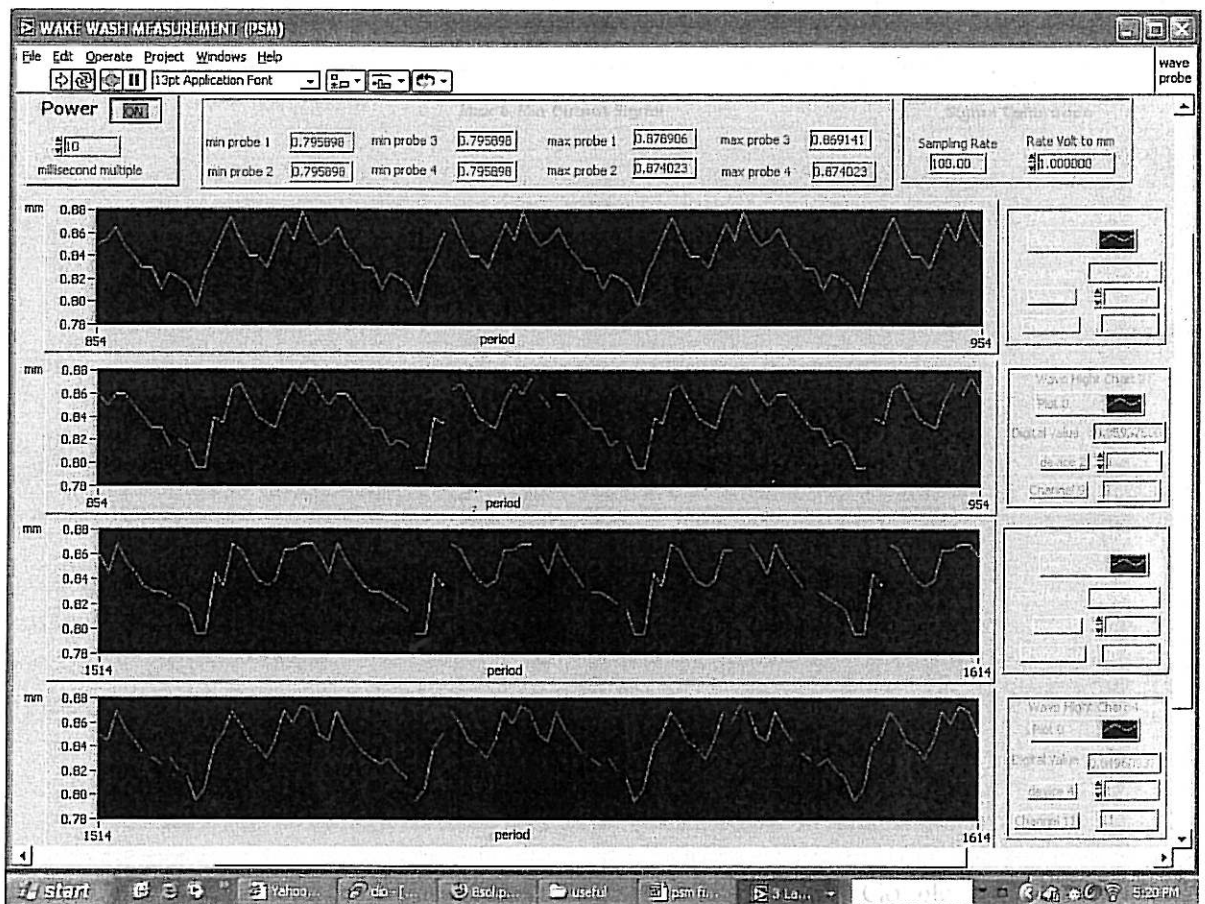


Figure 16: The front panel of wash measurement

with 4probe n max n min and file save all 4 probe final 1 with setting  
D:\PSM LABVIEW\useful\with 4probe n max n min and file save all 4 probe final 1 with setting  
Last modified on 3/22/2006 at 1:00 AM  
Printed on 4/13/2006 at 12:27 AM

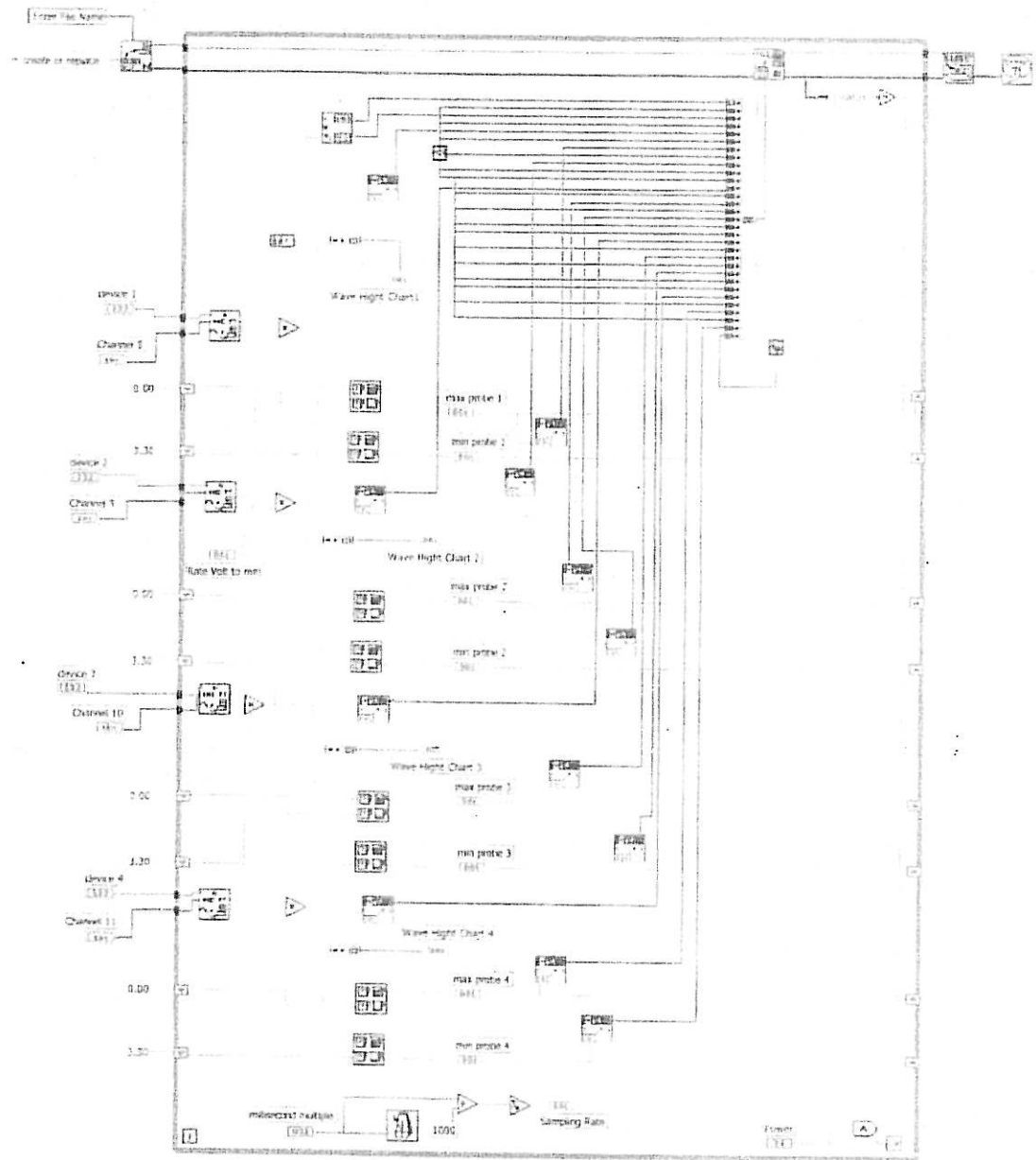


Figure 17: The block diagram of Wash measurement

When data acquisition is performed, the software needs to know the following information:

- Device number
- Channel that is being used
- Sampling Rate

Often LabVIEW is used to perform system simulations, since it contains many commonly used filter, digital signal processing, and statistical functions. LabVIEW compiles almost as fast as C or Matlab and therefore one can perform complete simulation within a vi. In addition to data input output, LabVIEW can access serial ports, parallel ports and GPIB cards to read data from instruments that have a GPIB interface.



## CHAPTER 5

### EXPERIMENT IN SHALLOW WATER

#### 5.1 Instrumentation and Data Acquisition setup

An array of 4 twin wires resistance probes was used to measure the wash wave profiles produced by the ship model (Harbour Patrol Craft) with different depth Froude number. These were connected via a 4 channel to a laptop for data acquisition. Table 2 show the channel was used corresponding to wave probe number. Wave probe was attach at tank beam located at optimum longitudinal position for longest possible wave trace which is approximately 7.3 meter from first enter of shallow water platform. Figure 18 and figure 19 illustrates the probes arrangement by using an arm and the distance from the sailing line is given in table 3.

Table 4 shows the details of parallel wire resistance wave probes specification measuring the surface elevation in the model tank. The wires were fed with direct current (DC) with a 3.19 Volts. An amplifier measured the drop of voltage at two resistors, which were connected in line with both wires of the probe. This signal was rectified into a pulsing direct current and smoothed by a filter. An analog/digital converter identified this signal. The package LabView® was used for data acquisition. The values were read from the DAQ Card 700 at a frequency of 50 Hz. All digital values was automatically write to Microsoft excel. Table 5 show the command used for data display at Microsoft excel when LabView read the data and written to Microsoft excel.

Table 2: Probe No. corresponding to channel

| <i>Probe No.</i> | <i>Channel</i> |
|------------------|----------------|
| probe 1          | 8              |
| probe 2          | 9              |
| probe 3          | 10             |
| probe 4          | 11             |

Table 3 : The wave probe position

| <i>Probe No.</i> | <i>Distance from sailing line</i> | <i>y/L</i> |
|------------------|-----------------------------------|------------|
| Probe 1          | 0.8 m                             | 0.53       |
| Probe 2          | 1.0 m                             | 0.66       |
| Probe 3          | 1.2 m                             | 0.79       |
| Probe 4          | 1.4m                              | 0.93       |

Table 4: Details of probe specification

|                       |                 |
|-----------------------|-----------------|
| Probe length          | 300 mm          |
| Probe wire diameter   | 0.5 mm          |
| Probe wire separation | 12.5 mm         |
| Probe wire material   | stainless steel |
| Cable length          | 2 meter         |

Table 5: Command used for data display at excel

| <i>Column No.</i> | <i>Description</i> | <i>Format</i> |
|-------------------|--------------------|---------------|
| Column 1          | date               | M/D/Y         |
| Column 2          | time               | H:M:S         |
| Column 3          | probe 1 value      | 6 decimal     |
| Column 4          | max value probe 1  | 6 decimal     |
| Column 5          | min value probe 1  | 6 decimal     |
| Column 6          | space              | -             |
| Column 7          | probe 2 value      | 6 decimal     |
| Column 8          | max value probe 2  | 6 decimal     |
| Column 9          | min value probe 2  | 6 decimal     |
| Column 10         | space              | -             |
| Column 11         | probe 3 value      | 6 decimal     |
| Column 12         | max value probe 3  | 6 decimal     |
| Column 13         | min value probe 3  | 6 decimal     |
| Column 14         | space              | -             |
| Column 15         | probe 4 value      | 6 decimal     |
| Column 16         | max value probe 4  | 6 decimal     |
| Column 17         | min value probe 4  | 6 decimal     |

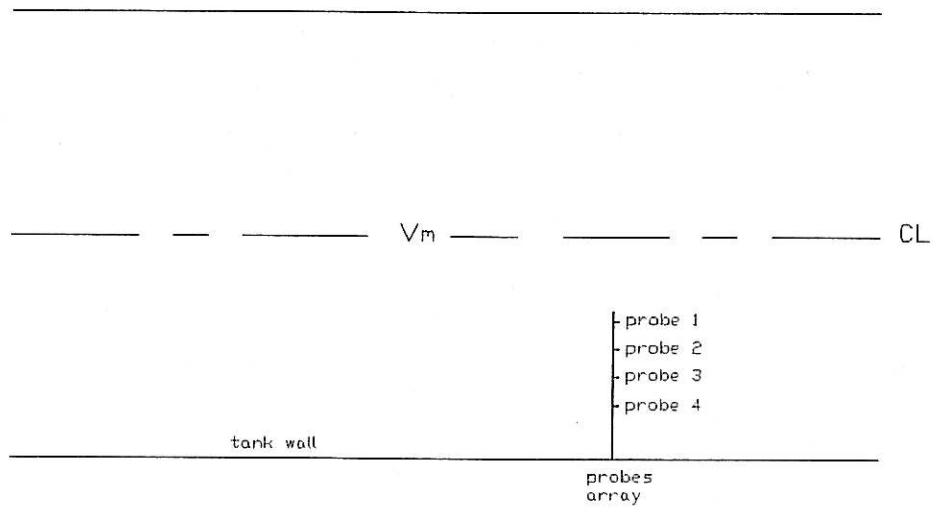


Figure 18: Schematic drawing of probe arrangement at tank

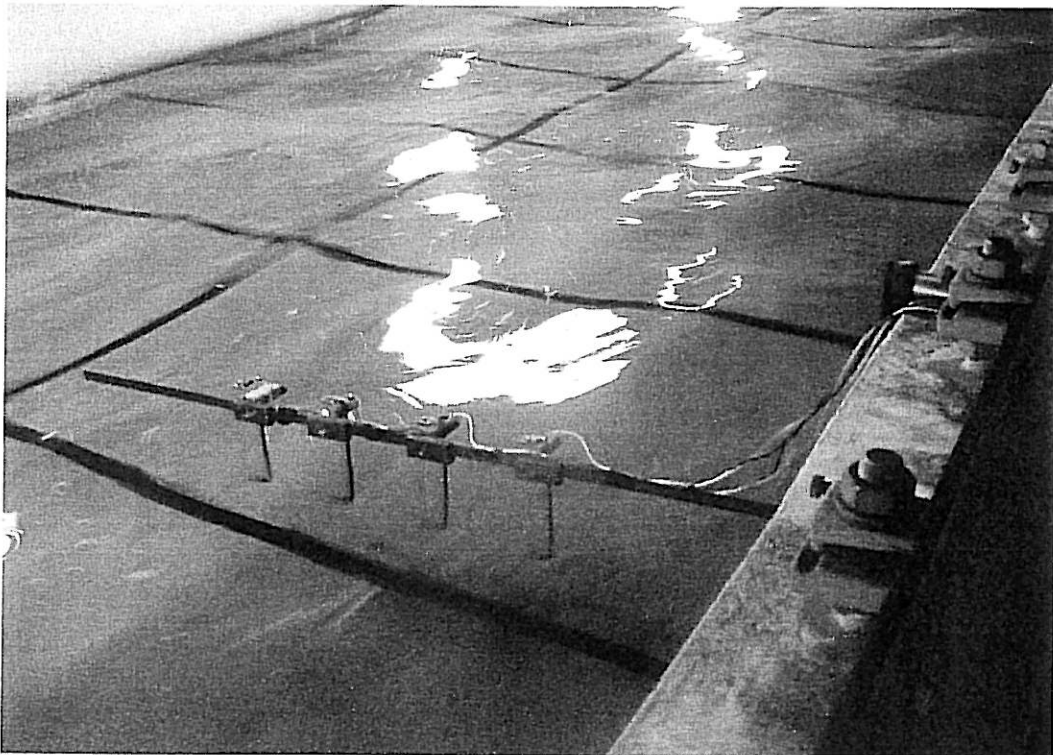


Figure 19: Picture of probe Arrangement

## 5.2 Test conditions and data presentation of result

Experiment to investigate wake wash from patrol craft were conducted in calm water with difference depth Froude number at Towing Tank of Marine Technology Laboratory UTM, Skudai. During model test, tank water temperature is 22.7 °C. Details of towing tank are shown in table 6. Model condition at 0.0072 m trim by bow was selected to prevent disturbance coming from water sprinkling. During the model tests to measure the wash, resistance, heave and trim were also recorded by D.A.A.S at towing carriage. All other data was recorded by LabView software which integrates with wave probe, signal conditioning unit and laptop. Figure 20 show the developed computerized data acquisition system.

Table 6 : Towing Tank Details

|                               |       |
|-------------------------------|-------|
| Length                        | 120 m |
| Useful Length                 | 90 m  |
| Breadth                       | 4 m   |
| Depth                         | 2.5 m |
| Max. Carriage Speed           | 5 m/s |
| Shallow Water Platform Depth  | 0.3 m |
| Shallow Water Platform Length | 16 m  |

The model was tested for different speed in calm water corresponding to the Depth Froude Number,  $F_{nh}$  0.6 to 1.4. Table 7 show the condition of model tested.

Table 7: Test Conditions

| <b>Fnh</b>         | 0.6  | 0.7  | 0.8  | 0.9  | 1    | 1.1  | 1.2  | 1.3  | 1.4  |
|--------------------|------|------|------|------|------|------|------|------|------|
| <b>Vm</b><br>(m/s) | 1.03 | 1.20 | 1.37 | 1.54 | 1.72 | 1.89 | 2.06 | 2.23 | 2.40 |

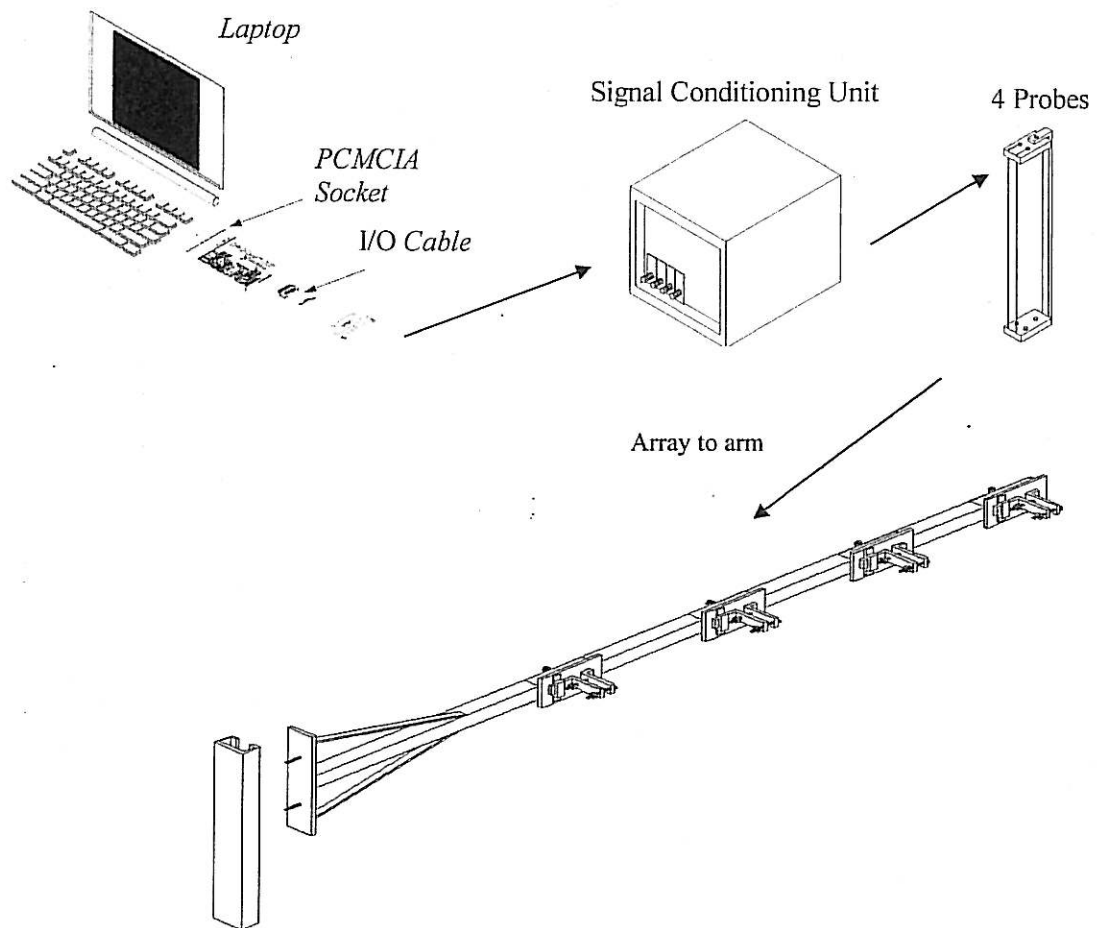


Figure 20: Schematic of wash measurement system

### 5.3 Model Preparation

A Harbour Patrol Boat model (MTL 0029) in figure 21 was selected for wake wash investigations. It has a scale factor of 1: 8.75 of the real ship. The principle particular of the model and ship at test conditions are shown in table 8. The model is ballasted to the corresponding draft, centre of gravity and trim with respect to the full scale of the ship. All this preparation is done with the facilities available in the Marine Technology Laboratory.

Table 8: The principle particular of the model and full scale ship conditions used for investigation

|                     | Model                  | Ship                 |
|---------------------|------------------------|----------------------|
| LOA                 | 1.71 m                 | 15.0 m               |
| LBP                 | 1.44 m                 | 12.6 m               |
| LWL                 | 1.51 m                 | 13.2 m               |
| Breadth             | 0.48 m                 | 4.2 m                |
| Draught @ Amidship  | 0.111 m                | 0.975 m              |
| Draught @ Forward   | 0.119 m                | 1.038 m              |
| Draught @ Aft       | 0.104 m                | 0.911 m              |
| Trim                | 0.0072 m by Bow        | 0.063 m by Bow       |
| Displacement Volume | 0.02926 m <sup>3</sup> | 19.60 m <sup>3</sup> |
| LCG from AP         | 0.615 m                | 5.385 m              |
| KG                  | 0.223                  | 1.948 m              |
| Wetted Surface Area | 0.6668 m <sup>2</sup>  | 51.05 m <sup>2</sup> |
| Cb                  | 0.392                  |                      |
| Cp                  | 0.709                  |                      |
| Appendages          | Stern Wedge            |                      |
| Model Scale         | 1 : 8.75               |                      |

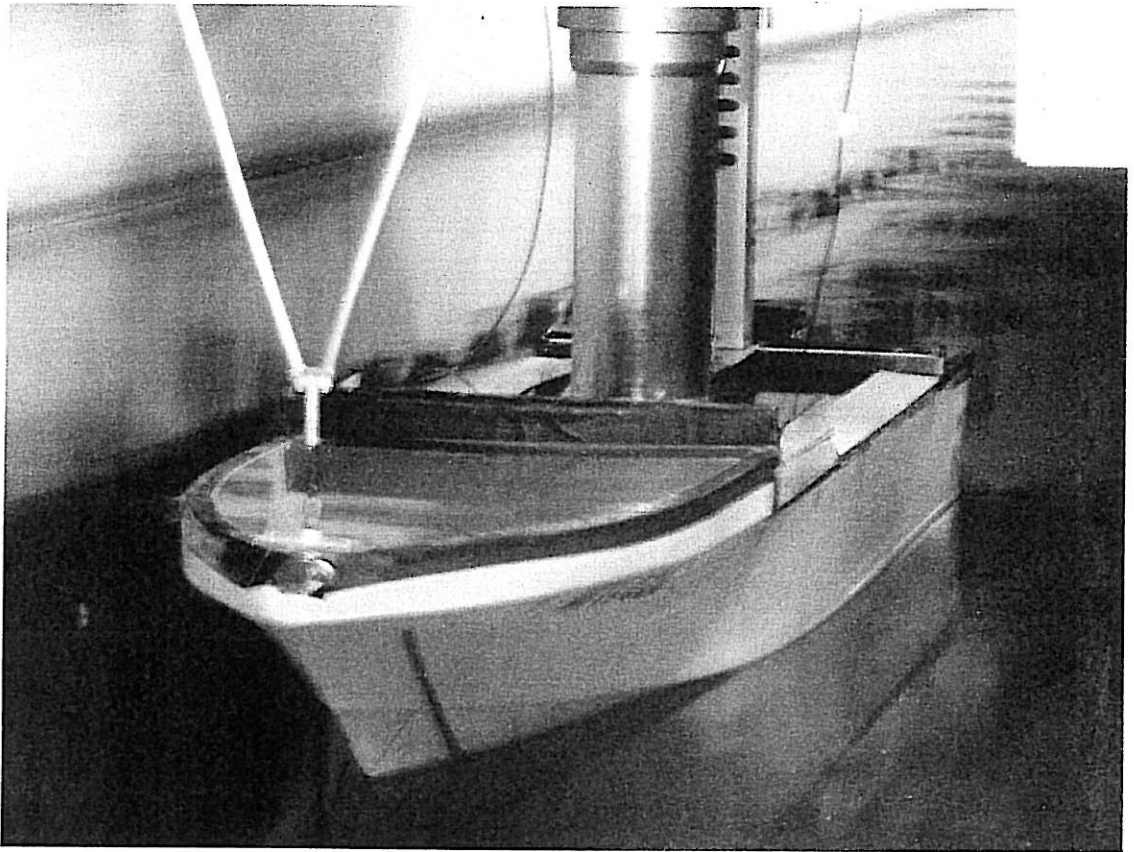


Figure 21: Model ready for testing

Model preparation show in table 8 is at initial condition, while at running condition, parameters for trim, draught, and length water line is vary corresponding to depth Froude number influence. Figure 22.1 and 22.2 show the heave and trim condition respectively at every depth Froude number when model at deep water and shallow water during tests. Varying in heave and pitch will describe the changing of draught and length water line at different depth Froude number.



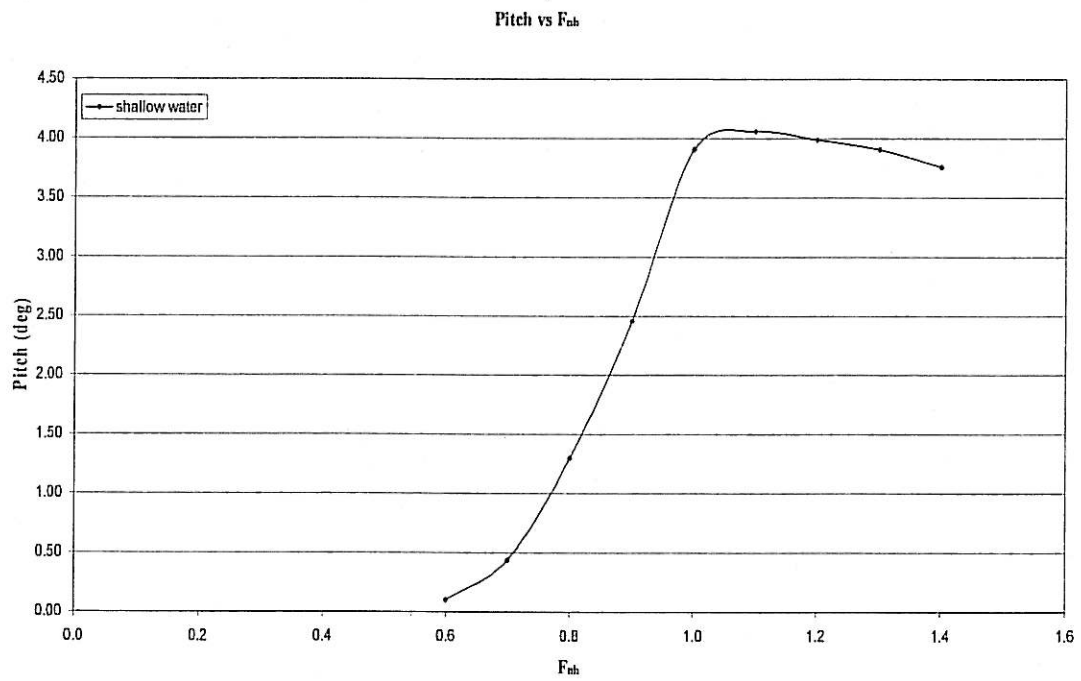


Figure 22.1: Model pitch condition during tests at difference  $F_{nh}$

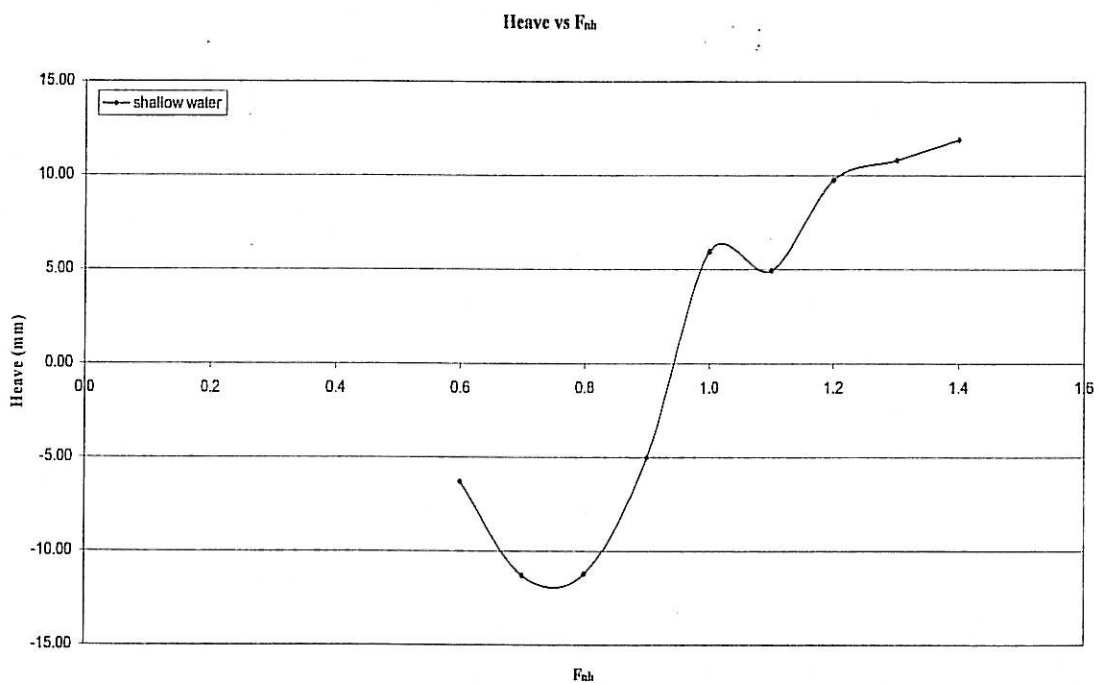


Figure 22.2: Model heave condition during tests at difference  $F_{nh}$

#### 5.4 Wave probe calibration method

Before experiment begins, wave probe should be calibrated to get the relationship between voltage heights of wave. The procedure below was follow for calibration.

- Probe was submerging into water to lower part as reference and then voltage was recorded.
- Move the probe or submerge 5cm down into water from reference then voltage was recorded.
- Repeat step above again for every 5cm until 15cm submerge.
- This task was presented in table 9
- Graph voltage vs. height was plotting to check the linearity of instrument.

Table 9: The calibration table for wave probe

| <i>Height (cm)</i> | <i>Voltage (Volt)</i> |                |                |                |
|--------------------|-----------------------|----------------|----------------|----------------|
|                    | <i>Probe 1</i>        | <i>Probe 2</i> | <i>Probe 3</i> | <i>Probe 4</i> |
| 0 (as a reference) | 2.6143                | 2.53465        | 2.5731         | 2.4832         |
| 5                  | 2.5413                | 2.4796         | 2.5113         | 2.4213         |
| 10                 | 2.4778                | 2.4101         | 2.4398         | 2.3498         |
| 15                 | 2.4197                | 2.3431         | 2.3857         | 2.2931         |

From calibration above, the relationship between voltage and height of wave can express in figure 23 to check the linearity of probe. The slope of the graph represents the changing of voltage (volt) per length (cm).

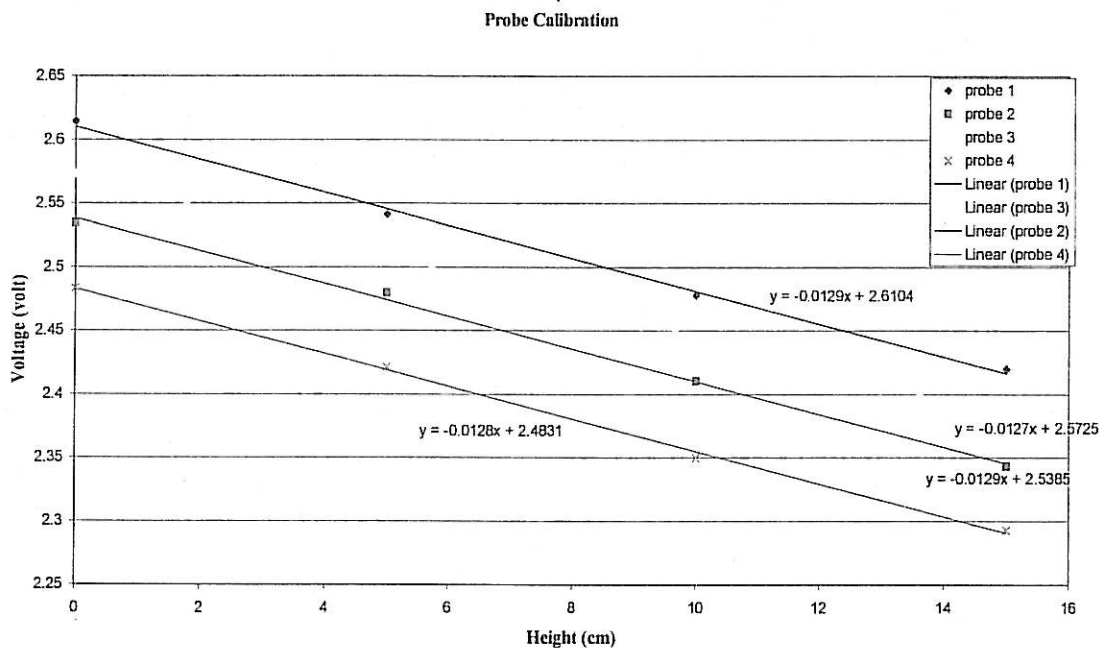


Figure 23: Probe calibration

Calibration also was carried out again when wave probe attached in the tank and at this time, the user zero was set before measuring wake wash. Three values was recorded when probe submerge between maximum and minimum level of wire probe length during this calibration. Figure 24 shows the value of calibration was done at tank. The slope of the graph represents the sensitivity of the instrument to changing in voltage (volt) per length (cm). From this graph, found that the probe sensitivity is 12.8mV per cm for average. From this sensitivity, the accuracy of this instrument to be  $\pm 0.6\text{mm}$  by using 12bit resolution. This accuracy will be increased by using higher resolution for DAQ Card.

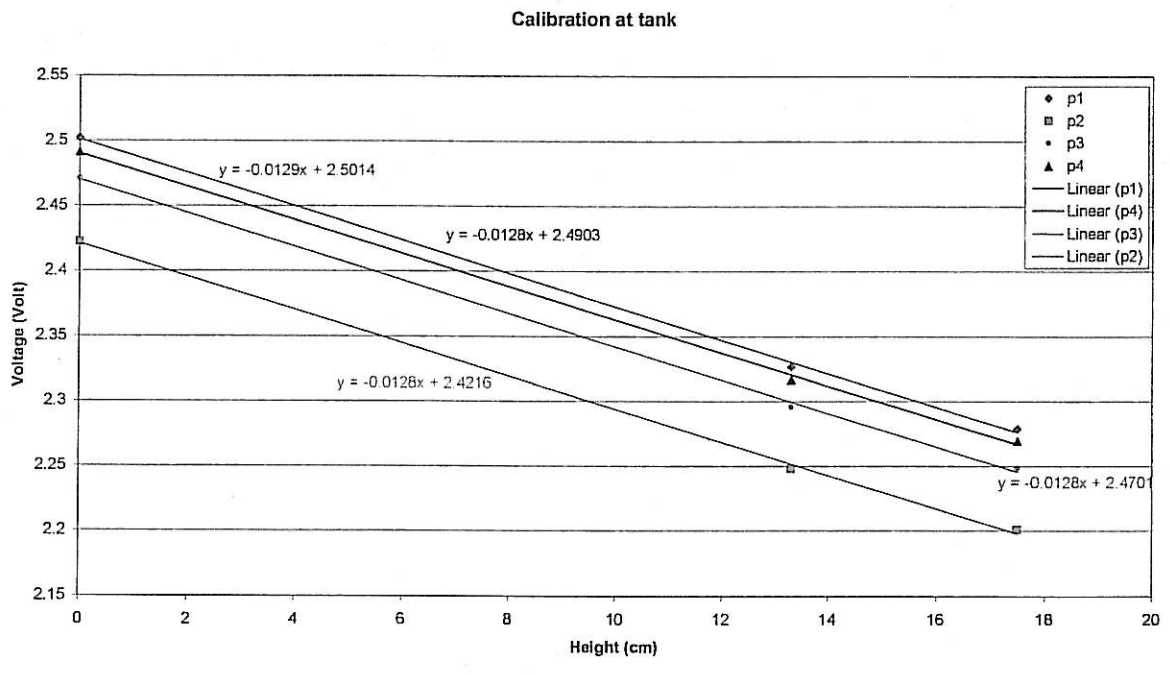


Figure 24: Calibration during experiment at tank

## 5.5 Result and discussion

There are several methods which can be used to analyze the measured data. The first approach utilizes the wave energy method, i.e the calculation of the energy of the wave system at the measuring position. The second approach is based on the maximum and minimum amplitude of the generated wave (or to find the highest wave in the measured data). This study only covers the second approach and the results are tabulated in table 12. The same information is presented in graphical format in figure 25. These figures show a plot of the maximum wave height for the model as function of  $F_{nh}$  at 4 different probe locations. It is obvious from this figure that the largest waves are produced at depth Froude number is near the so-called critical Froude number,  $F_{nh} \approx 0.9$ . The result was validating with theoretical approach equation in table 1 produce by Kriebel, Seelig and Judge (2001). However, these formulas are only relevant for  $F_{nh}$  up to 0.8, and the predictions below  $F_{nh}$  of 0.3 will be less accurate. Table 14 shows the results was calculated from theoretical approach. The same result was illustrated in figure 25.

Table 10 and 11 shows the data from D.A.A.S for total ship resistance, pitch and heave at shallow water and deep water respectively. Figure 26.1 and 26.2 show the total model resistance plotted against depth Froude number and model speed respectively in deep and shallow waters. It can be seen that model resistance rising rapidly as the shallow water critical speed was approach. In this figure also, it can be seen that there was an increase in resistance in shallow water at sub-critical speeds, rising to a peak just below the depth Froude number,  $F_{nh} = 1.1$ , but at super critical speeds a reduction in resistance was obtained when compared with the value in deep water at the same speed.

Figure 27 and 28 show the heave and pitch at shallow water and deep water respectively. It can be seen that pitch angle rising rapidly and heave found to life up as the shallow water critical speed was approach. From this figure, it can be conclude that when ship achieve critical speed it try to plan as a planning craft characteristic and this

condition will influence the length-to beam ratio ( $L_{WL}/B$ ) simultaneously wash height because wash height are inversely proportional to length-to beam ratio.

Figure 30 shows the relationship between the divergence of the leading wave crest divergence and the depth Froude number. It was obtained using the four wave probe at different distance from sailing line. Knowing the sampling rate of data recorded from LabView was possible to calculate the distance “d” illustrate in figure 29. The values of data collected for crest traveling from probe 1 to probe 4 can use to define the distance “d”. The wave angles were then calculated using these “d” values at difference depth Froude number by using formula (5.1.1). By using the mathematical model in (2.1.1) and (2.1.2), theoretical values were also calculated for each experimental point. The correlation with the experimental data is quite good. The mathematical model predicts a definite dependence of this angle with water depth as well as depth Froude number.

Table 10: Result from D.A.A.S for shallow water (0.3m water depth)

| <b>Vm<br/>(m/s)</b> | <b>Fnh</b> | <b>Fx (N)</b> | <b>Pitch<br/>(deg)</b> | <b>Heave<br/>(meter)</b> |
|---------------------|------------|---------------|------------------------|--------------------------|
| 1.03                | 0.6        | 4.09          | 0.10                   | -0.0063                  |
| 1.20                | 0.7        | 7.14          | 0.44                   | -0.0113                  |
| 1.37                | 0.8        | 11.90         | 1.30                   | -0.0112                  |
| 1.54                | 0.9        | 16.20         | 2.46                   | -0.0050                  |
| 1.72                | 1.0        | 19.70         | 3.91                   | 0.0059                   |
| 1.89                | 1.1        | 20.20         | 4.06                   | 0.0050                   |
| 2.06                | 1.2        | 20.60         | 3.99                   | 0.0098                   |
| 2.23                | 1.3        | 21.00         | 3.91                   | 0.0108                   |
| 2.40                | 1.4        | 22.40         | 3.76                   | 0.0119                   |

Table 11 : Result from D.A.A.S for deep water

| <b>Vm<br/>(m/s)</b> | <b>Fnh</b> | <b>Fx (N)</b> | <b>Pitch<br/>(deg)</b> | <b>Heave<br/>(meter)</b> |
|---------------------|------------|---------------|------------------------|--------------------------|
| 1.03                | 0.6        | 4.19          | 0.08                   | -0.0051                  |
| 1.20                | 0.7        | 6.86          | 0.24                   | -0.0086                  |
| 1.37                | 0.8        | 8.03          | 0.08                   | -0.0064                  |
| 1.54                | 0.9        | 10.70         | 0.21                   | -0.0088                  |
| 1.72                | 1.0        | 14.17         | 0.97                   | -0.0114                  |
| 1.89                | 1.1        | 18.80         | 2.13                   | -0.0150                  |
| 2.06                | 1.2        | 22.00         | 3.13                   | -0.0130                  |
| 2.23                | 1.3        | 23.60         | 3.71                   | -0.0100                  |
| 2.40                | 1.4        | 25.10         | 3.98                   | 0.0070                   |

Table 12: Maximum wash result from LabView

|            | <b>probe 1<br/>y/L = 0.53</b> | <b>probe 2<br/>y/L = 0.66</b> | <b>probe 3<br/>y/L = 0.79</b> | <b>probe 4<br/>y/L = 0.93</b> |
|------------|-------------------------------|-------------------------------|-------------------------------|-------------------------------|
| <b>Fnh</b> | <b>Hmax<br/>(mm)</b>          | <b>Hmax (mm)</b>              | <b>Hmax<br/>(mm)</b>          | <b>Hmax (mm)</b>              |
| 0.6        | 9.86                          | 9.18                          | 7.65                          | 6.19                          |
| 0.7        | 18.78                         | 17.26                         | 15.21                         | 13.32                         |
| 0.8        | 31.49                         | 29.62                         | 27.25                         | 23.34                         |
| 0.9        | 44.72                         | 42.43                         | 39.23                         | 35.14                         |
| 1.0        | 35.27                         | 33.13                         | 30.88                         | 26.75                         |
| 1.1        | 33.15                         | 31.02                         | 27.53                         | 23.97                         |
| 1.2        | 35.86                         | 32.84                         | 29.97                         | 25.83                         |
| 1.3        | 36.83                         | 33.58                         | 30.34                         | 26.36                         |
| 1.4        | 36.97                         | 35.84                         | 34.86                         | 32.92                         |

Table 13: Predicted of divergent angle from experiment

| <b>F<sub>nh</sub></b> | <b>Divergent Angle, <math>\theta</math></b> |
|-----------------------|---|
| 0.6                   | 32.13                                       |
| 0.7                   | 31.73                                       |
| 0.8                   | 30.75                                       |
| 0.9                   | 25.37                                       |
| 1.0                   | 12.86                                       |
| 1.1                   | 24.38                                       |
| 1.2                   | 32.48                                       |
| 1.3                   | 35.82                                       |
| 1.4                   | 41.37                                       |

Table 14: Theoretical approach for maximum wash

|                       | <b>probe 1</b><br><b>y/L = 0.53</b>   | <b>probe 2</b><br><b>y/L = 0.66</b>   | <b>probe 3</b><br><b>y/L = 0.79</b>   | <b>probe 4</b><br><b>y/L = 0.93</b>   |
|-----------------------|---------------------------------------|---------------------------------------|---------------------------------------|---------------------------------------|
| <b>F<sub>nh</sub></b> | <b>H<sub>max</sub></b><br><b>(mm)</b> | <b>H<sub>max</sub></b><br><b>(mm)</b> | <b>H<sub>max</sub></b><br><b>(mm)</b> | <b>H<sub>max</sub></b><br><b>(mm)</b> |
| 0.6                   | 12.94                                 | 12.03                                 | 11.33                                 | 10.73                                 |
| 0.7                   | 25.91                                 | 24.09                                 | 22.68                                 | 21.48                                 |
| 0.8                   | 46.77                                 | 43.47                                 | 40.94                                 | 38.77                                 |

Table 15: Theoretical approach for divergent angle

| <b>F<sub>nh</sub></b> | <b>Divergent Angle, <math>\theta</math></b> |
|-----------------------|---|
| 0.6                   | 34.98                                       |
| 0.7                   | 34.30                                       |
| 0.8                   | 32.07                                       |
| 0.9                   | 24.64                                       |
| 1.0                   | 0.00  |
| 1.1                   | 24.62                                       |
| 1.2                   | 33.56                                       |
| 1.3                   | 39.72                                       |
| 1.4                   | 44.42                                       |



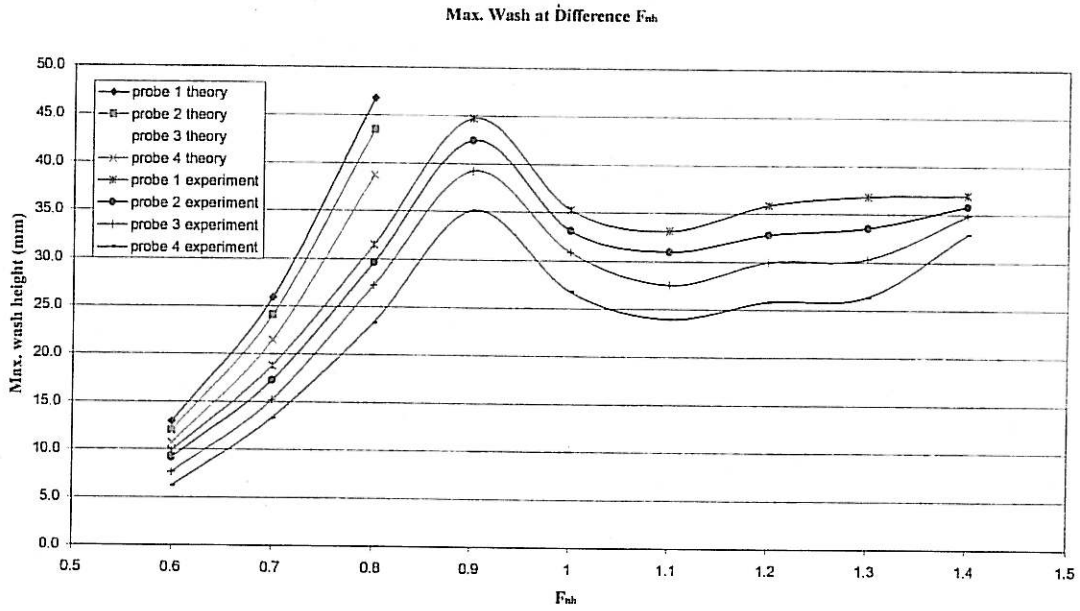


Figure 25: Predicted from experiment and theoretical approach of maximum wash

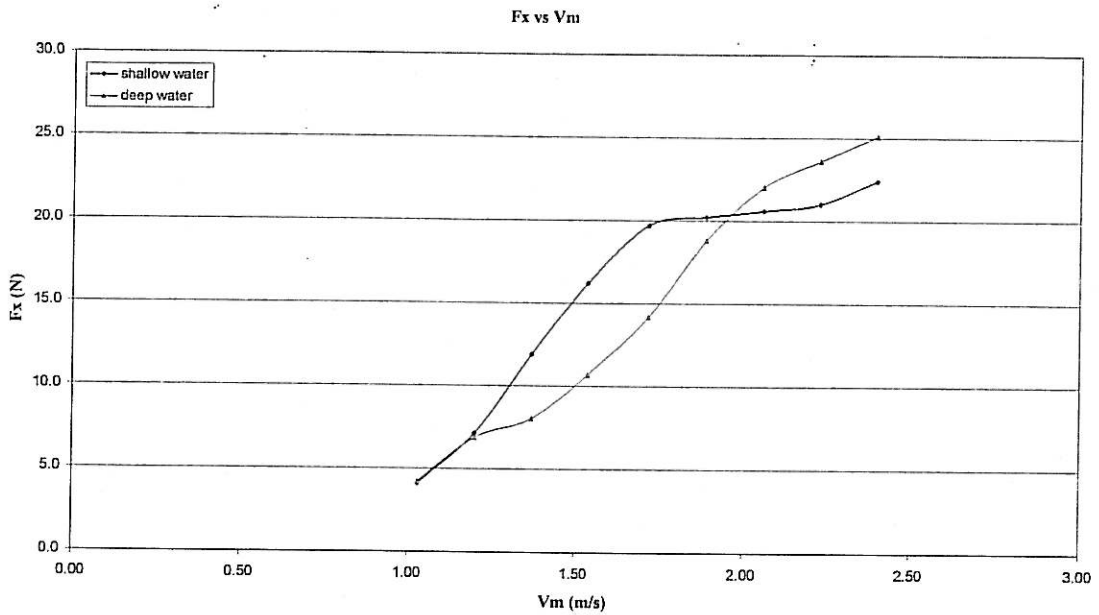


Figure 26.1: Resistance characteristic against model speed

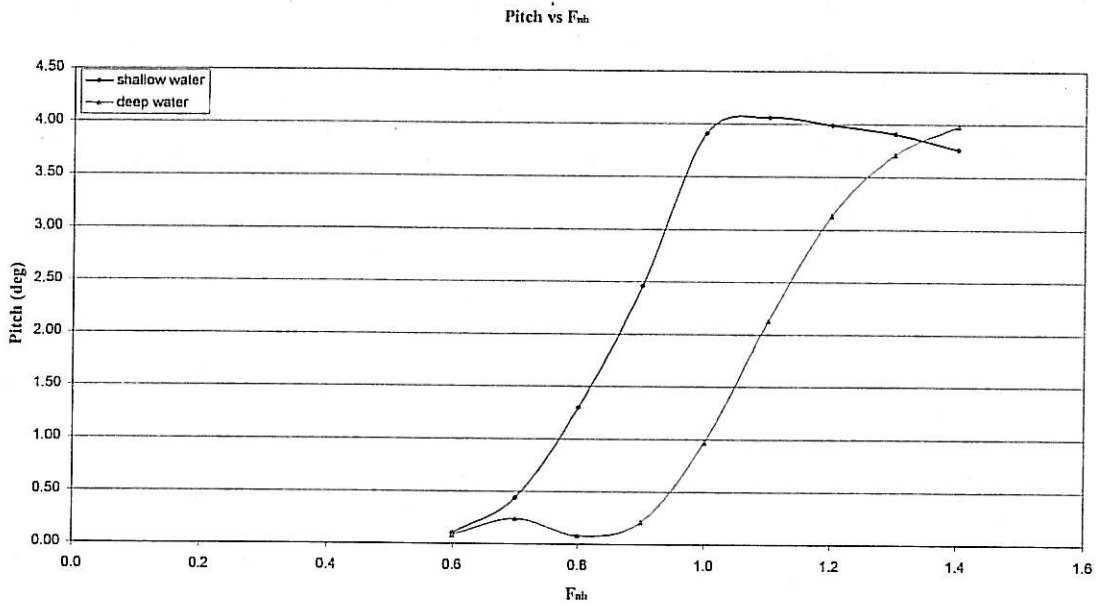


Figure 28: Pitch characteristic against depth Froude number

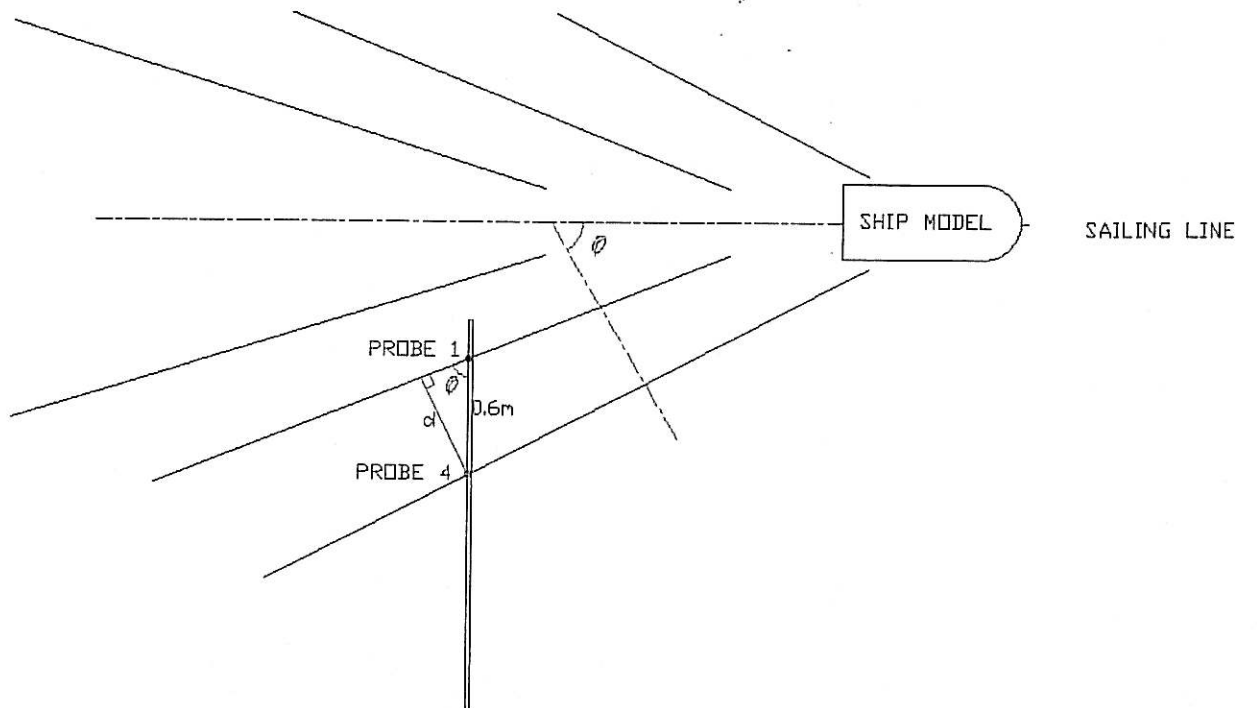


Figure 29: Divergent angle illustration

LabView will write data at every 0.01-second by using 100 sampling rate. From this, the time crest travel from probe 1 to probe 4 can be determine. Before this, the relationship between time and distance should be fine first. From  $\lambda = \frac{gT^2}{2\pi} \tanh \frac{2\pi h}{\lambda}$  the value of the  $\lambda$  can be determine. This value was representing by the data collected along the first crest to second crest at each one of probe. From this data, the time for wave length,  $\lambda$  travel can be determined. The time for wave travel along the  $\lambda$  was compare with the value of  $\lambda$  (meter). Then the relationship between the time and distance (time-length ratio) can be estimate. From this relationship, “d” value can be estimate from the frequently of data collected for the same crest travel from first probe to last probe. Then the time was multiply by the time-length ratio to get “d” value. Then the equation below can be use to get the  $\theta$  from “d” value.

According to figure 29, divergent angle,  $\sin \theta = \frac{d}{0.6}$

$$\theta = \sin^{-1} \frac{d}{0.6} \quad (5.1.1)$$

All this procedure was repeated for every depth Froude number to get divergent angle at different depth Froude number.

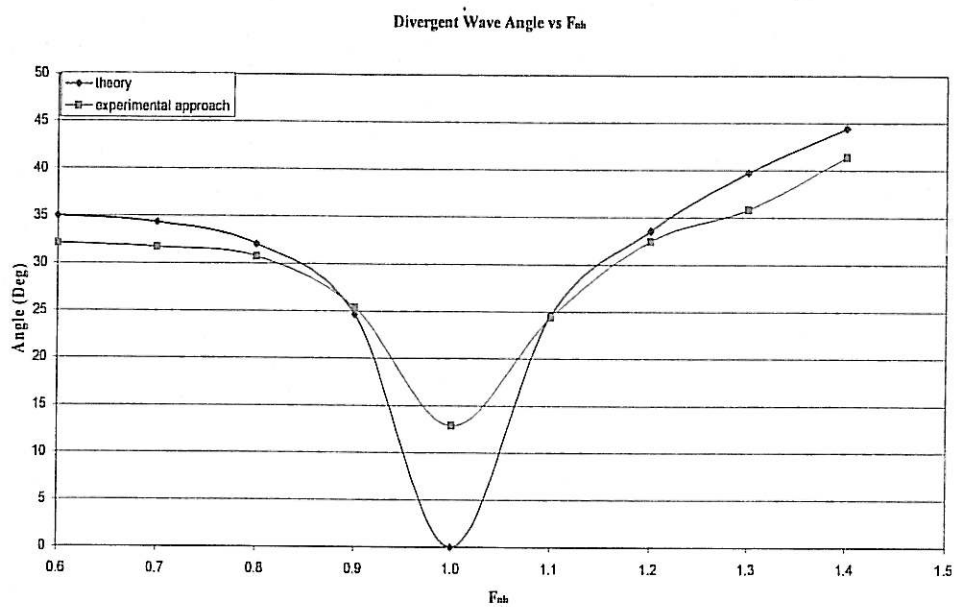


Figure 30: Predicted from experiment and theoretical approach of divergent angle

## 6.2 Recommendation

This study has quantified and analysed the characteristics of the wake wash generated by the Harbour Patrol Craft but there is still spaces left to improve the result. The following recommendations are made for further study and for better improvement:

- Difference method of measuring by placing wave probe at difference location along sailing line.
- As the towing tank facility in the Marine Technology Laboratory is limited by several aspects such as shallow water platform too short, so that when vessel transiting from deep water to shallow water wash disturbance occurs during measurement especially at higher depth Froude number. This will contributes to measure exact wake wash.
- Using computer program such as ship flow to validate all the result collected from experiment.
- Improve the instrumentation developed to reduce the noise as low as possible.

## CHAPTER 6

### CONCLUSION AND RECOMMENDATION

#### 6.1 Conclusion

The objective of this thesis is to investigate wake wash characteristic from Harbour Patrol Craft (MTL 0096) was done successfully by using developed instruments and water wave probe with facilities available at towing tank and towing carriage in Marine Laboratory, Universiti Teknologi Malaysia. The pattern of the wash wave system has been measured for different depth and length Froude numbers and compared with theoretical predictions. The following has been concluded;

- Result analysis show that the agreement between the theoretical and experimental curve pattern is reasonably good.
- Wake wash characteristic generated by traveling vessel is largely dependent on the depth Froude number.
- The hump speed was achieve at depth Froude number,  $F_{nh} \approx 0.9$

From this experiment, the characteristics of wake wash produce from patrol craft was observe and can be adopted in real phenomena. All the data produced is useful for further study to improve wake wash produced in design of patrol craft and for decide a standard service speed for patrol craft operation in critical area.

## REFERENCES

1. 'Wake Wash & Motion Control', Presented at The Royal Institution of Naval Architects International Conference on Hydrodynamics of High Speed Craft, 7-8 November 2000, London. Papers.
2. STAN STUMBO, KENNETH FOX, FRANK DVORAK, and LARRY ELLIOT, 'The Prediction, Measurement, and Analysis of Wake Wash from Marine Vessels', Marine Technology Vol.36, No.4, Winter 1999.
3. Whittaker Trevor J.T., "An Experimental Investigation of the Physical Characteristics of Fast Ferry Wash", 2nd International Euro-Conference on High-Performance Marine Vehicles HIPER'01, Coastal Engineering; Queen's University Belfast, 2001.
4. Stan Stumbo, Kenneth Fox and Larry Elliott, 'An Assessment of Wake Wash Reduction of Fast Ferries at Supercritical Froude Numbers and at Optimized Trim'.
5. STAN STUMBO, KENNETH FOX, and LARRY ELLIOT, "Hull Form Considerations in the Design of Low Wake Wash Catamarans", Presented at the SNAME International FAST '99 Conference, Seattle, WA, USA, August, 1999.
6. M/V CONDOR EXPRESS WAKE WASH MEASUREMENT TRIALS, February 22, 2002, Prepared by Fox Associates, Naval Architects & Water Transportation Consultants, 14100 Madison Avenue N.E. • Bainbridge Island, WA. 98110.
7. Michael Bruno, Brian Fullerton and Raju Datla, "Ferry Wake Wash in NY/NJ Harbor" (07030 TECHNICAL REPORT SIT-DL-02-9-2812) Prepared for New Jersey Department of Transportation under FAO# 9428119, October 2002 (SIT Davidson Laboratory Project No. 525400).
8. 'Wake Wash Study for Calder Harbour Channel', Presented by DHI Water & Environment.

9. Final Report of MCA Research Project 457, 'A Physical Study of Fast Ferry Wash Characteristics in Shallow Water'.
10. [http://www.ukmarinesac.org.uk/activities/ports/ph3\\_2\\_1.htm](http://www.ukmarinesac.org.uk/activities/ports/ph3_2_1.htm)
11. <http://www.cormon.com/catalog/techpres.htm>
12. Macfarlane G.J., Renilson M.R. (Australian Maritime College), "Wave Wake – A Rational Method of Assessment", RINA, Conference on Coastal Ship and Inland Waterways, London, February, 1999.
13. Dr M.B Single, "Wake Wash Measurements in Tory Channel, Marlborough Sounds", Final Technical Note September 2001 presented by DHI Water & Environment.
14. Whittaker, T.J.T., Doyle, R., Elsaesser, B., 2000; A study of leading long period waves in fast ferry wash, Proc. Hydrodynamics of High Speed Craft – wake wash and motions control, RINA, London, Nov. 2000, paper 7.
15. Tao Jiang, Rupert Henn & Som Deo Sharma, "Wash Waves Generated by Ship Moving on Fairways of Varying Topography, 24<sup>th</sup> Symposium on Naval Hydrodynamics Fukuoka, Japan, 8-13 July 2002.
16. M.P Abdul Ghani, "Design Aspects of Catamaran Operating at High Speed in Shallow Water", thesis for the degree of Doctor of Philosophy, University of Southampton, June 2003.